Geophysical Journal (1988) **93,** 485–504

Rheological modelling and deformation instability of lithosphere under extension

Gianna Bassi and Jean Bonnin

Laboratoire de Géodynamique, Institut de Physique du Globe, 5 rue René Descartes, 67084 Strasbourg Cedex, France

Accepted 1987 November 13. Received 1987 November 13; in original form 1986 December 15

SUMMARY

Continental break-up, which precedes oceanic accretion, probably results from an unstable extension of the lithosphere, analogous to necking of metals when they are submitted to tension. By reason of complexity of the rheology, no conclusion about lithospheric extension stability may be reached by an *a priori* analysis. We thus examine directly the evolution, when the lithosphere is stretched, of lateral inhomogeneities, represented in our example by small-scale variations of thickness. The rheological model is derived from the hypotheses of Brace & Kohlstedt (1980) and is consistent with the results of rock mechanics. The lithosphere consists of three or four layers of varying thicknesses and mechanical properties. The brittle upper crust and, eventually, the brittle part of the mantle are assimilated to perfectly plastic media and are described, in a state of uniform extension, by a constant viscosity. In the lower crust and ductile mantle lithosphere, the effective viscosity is supposed to be exponential. The mechanical model relies on a perturbation method developed by Fletcher & Hallet (1983), among others. Contrary to previous published results, no unstable behaviour of the lithosphere is observed unless the latter is more dense than the asthenosphere, in which case a gravitational instability may develop. This discrepancy can be explained by differences in assumptions concerning the variation of strength in the lithosphere, as yet poorly constrained by the data. We observe a great sensitivity of the results to the strength stratification and to the artificial discontinuities of density or viscosity implied by the models.

Key words: boudinage, lithosphere, necking, rheology, strength envelope, stretching instabilities

INTRODUCTION

There is a general agreement that extension of continental lithosphere is one of the principal mechanisms responsible for sedimentary-basin and continental-margin formation. In the latter case, the deformation leads to continental break-up and oceanic accretion. So far, the cause of extension and details of the rheological response during extension are poorly understood. Most of the proposed models (see e.g. Royden & Keen 1980; Cochran 1983), derived from the model of McKenzie (1978), give a purely geometrical description of the deformation; the others suppose that it is uniform throughout the plate and over the extending region. According to these models, the total lithospheric extension should amount to several hundreds of per cent to explain the observed subsidence of basins and margins (Keen & Barrett 1981; Beaumont, Keen & Boutilier 1982; Foucher *et al.* 1982).

Several authors (Kusznir & Park, Vink *et al.* 1984; Sawyer 1985) have paid particular attention to lithospheric strength and have evaluated the average stress required to produce significant extensional deformation. Their estimates strongly depend on the rheological hypotheses adopted so that, because of the uncertainties concerning the exact rheology of the lithosphere, it is difficult to reach a firm quantitative conclusion. It seems, however, that a continental lithosphere with low surface heat-flow ($<60\,\mathrm{mW\,m^{-2}}$) will not show any significant deformation through geological time if the magnitude of the average stress applied over the lithosphere thickness is less than 1 kbar, as it is usually thought to be. On the contrary, in continental regions with high surface heat-flow ($>75\,\mathrm{mW\,m^{-2}}$), stress arising from plate boundary forces or isostatically compensated loads are sufficient to cause a lithospheric extension of several hundreds of per cent in a few tens of million years, as required by the sedimentary basin models (Kusznir & Park 1982).

The preceding results were obtained assuming that continental lithosphere undergoes uniform extension and deforms in a pure shear strain field. Obviously, this is essentially a convenient mathematical approximation since the deformed region is always of limited extent. The lateral

homogeneity of the deformation is particularly difficult to justify in the case of continental margins where it leads to rupture.

So far, little attention has been paid to the exact structure and geometry of the lithosphere resulting from extension, and no dynamical model has been proposed to explain it. Yet, a description of the geometry of the deformed region should allow determination of the initial vertical movements of the lithosphere, which are poorly described by the present models (see e.g. Royden & Keen 1980). Moreover, it could give some insight into the conditions in which the deformation leads to continental break-up.

Our limited knowledge of the rheology of the lithosphere is clearly one of the major difficulties of any mechanical approach. Several authors (Artemjev & Artyushkov 1971; Beaumont *et al.* 1982) have proposed an analogy between lithospheric extension and break-up, and necking of materials when submitted to tension. As yet, this idea has not been developed in a quantitative way though it is interesting in several respects, particularly as far as continental margin formation is concerned. When a test sample begins to neck, the deformation concentrates in a narrow part of the bar where it leads, sooner or later, to fracture. Several arguments suggest the existence of the same type of instability in the lithosphere before continental break-up: first, the limited width of certain margins, like the Provençal or Corsican ones (50 km after stretching), which is difficult to explain within the framework of a uniform extension model; second, the observation that continental rupture is not necessarily located symmetrically with respect to the structure formed during rifting and that rift structures are often preserved on only one of the conjugate margins (Keen 1981). This last observation suggests that a 'defect' or an inhomogeniety of the lithosphere (of thickness or composition for example) has localized the deformation in a zone where it proceeds catastrophically. The total amount of extension of the lithosphere before it starts to neck may depend on its exact mechanical and structural properties, as suggested by the variable width of the margins (between 100 and 300 km).

Our initial purpose was to investigate the possibility of necking of the lithosphere by comparison with the analyses made for other, simpler materials. To this end, we first specify the mechanical properties of lithospheric rocks or, at least, the model which best accounts for experimental results on rock mechanics. Then, we briefly examine how the general criteria of stability apply to lithospheric extension and show that they are inadequate for our discussion. Mindful of the impossibility of reaching a conclusion *a priori*, we try to show evidence for an eventual instability of continental stretching by a direct determination of the evolution of small lithospheric thickness inhomogeneities. Our approach is based on the method proposed by Fletcher & Hallet (1983) and Ricard & Froidevaux (1986) which has been principally applied to the analysis of the basin and range structure. We improve the preceding studies through the choice of the mechanical parameters: whereas Ricard & Froidevaux (1986) and, to a lesser extent, Zuber *et al.* (1986) fix them in a rather arbitrary way, we try to constrain them by our rheological model of lithosphere, in the limit of the approximations required by the method. Our conclusions differ significantly from the previous ones, as we shall see.

RHEOLOGICAL MODEL. GENERAL CONSIDERATIONS ABOUT STABILITY IN TENSION

It is well known that mechanical properties of rocks greatly depend on their mineralogy, on temperature and pressure conditions, and on the eventual presence of aqueous fluids. This variety of mechanical behaviour, associated with the lack of constraints about the variation of the parameters with depth, explains that any rheological model of the lithosphere can only be approximate. This is particularly true for continental lithosphere by reason of the mineralogical and compositional heterogeneity of the continental crust, its complex thermal history, and the lack of rheologies for representative crustal rocks (Kirby 1983).

Goetze & Evans (1979) and Brace & Kohlstedt (1980) have summarized the rheological properties of oceanic and continental lithosphere, respectively, in a way that is consistent with recent results on rock mechanics. In broad outline, we shall adopt the variation of rheology with depth suggested by these models, with some simplifications that allow a much simpler mathematical formulation of the dynamical problem while respecting the main features of the rheological models.

Brace & Kohlstedt (1980) assume, as in other studies, that the rheology of olivine determines the mechanical properties of the upper mantle, whereas that of quartz controls the continental crust. While this is probably a reasonable assumption for the upper mantle, the use of quartz rheology for continental crust is questionable because of its mineralogical heterogeneity and will probably represent a lower bound to continental-crust strength (Vink *et al.* 1984; Zuber *et al.* 1986).

Brittle regime

In the brittle regime, Goetze & Evans (1979) first suggested that the behaviour of both the crust and the mantle is controlled by the possibility of sliding on pre-existing faults. The corresponding Byerlee's friction law is largely insensitive to the strain rate, temperature and nature of the material, but is highly sensitive to the effective pressure (lithostatic pressure minus pore pressure). If this law is recast into a failure-stress versus depth relation, it implies an approximately linear increase of failure stress with depth of burial (see Appendix B), with a rate of increase depending on the fluid pore pressure. Assuming that, in a fractured rock, fractures of all orientations exist, once the principal stresses reach the values given by Byerlee's law frictional sliding occurs somewhere; if the stresses are less, the deformation is purely elastic. Stresses predicted by Byerlee's law therefore represent the maximum permissible stresses in the brittle layer. This result can be compared with *in situ* measurements and appears to be consistent with experimental observations to about 4 km depth (Brace & Kohlstedt 1980; Kirby 1983). Extrapolation of this behaviour below this depth is more speculative as rocks may not be as fractured at depth as they are at the surface, and frictional resistance may not be accounted for properly by Byerlee's law. Even assuming that the extrapolation is valid, the increase of failure stress with depth is very sensitive to the pore-pressure level, which is in turn very poorly constrained.

This description of the crust-and-mantle brittle regime is quite similar to a perfectly plastic behaviour and the analogy has been extensively used to study plate flexure, particularly at subduction zones (see Kirby (1983) for a review). It implicitly assumes that the layer can be considered to deform as a continuous medium, which is reasonable if the fault spacing is much smaller than the length scale of the structures. Of course, this approach of brittle behaviour is a very indirect one and can be questioned. It can be viewed as an end member of a series of models giving variable importance to slip on discrete faults. While the consequences of this approximation should clearly be tested, we felt that the perfectly plastic model was appropriate for our first-order general analysis.

Ductile regime

The high-temperature ductile regime of olivine (above 1000 °C) has been fairly well explored by experimental work on single crystals and the results of individual analyses generally converge. In representative lithospheric conditions (stresses between 10 bar and 1 kbar), dislocation creep appears to be the dominant deformation mechanism. It corresponds to a power-law fluid behaviour and is highly temperature-dependent, as are most of the diffusion-controlled processes. The relationship between the principal stresses σ_1 and σ_3 and the strain rate $\dot{\varepsilon}$ has the form:

$$\dot{\varepsilon} = A(\sigma_1 - \sigma_3)^n \exp\left[-\frac{Q}{RT}\right]$$

where A, Q and n are material properties. For olivine, the stress exponent n is close to 3.

At lower temperatures, appropriate to oceanic or sub-cratonic upper mantle, stresses above 1 kbar are required to deform olivine crystals. Under these conditions, other deformation mechanisms are likely to become predominant. In their analysis, Goetze & Evans (1979) consider Dorn creep, which is also strongly non-linear and temperature dependent, to be the dominant mechanism for stresses above 2 kbar. However, this low-temperature behaviour of olivine is not well known yet and semi-brittle processes may be equally important (Kirby 1983). Because of these uncertainties and the generally 'warm' geotherms used in our analysis, which make this strong upper mantle very thin, we have not considered this low-temperature behaviour. As a consequence, the stresses involved in the construction of the strength envelope are likely to be overestimated whenever they exceed 2 kbar.

Our current understanding of quartz ductile behaviour is far more incomplete and appears to be critically dependent on the water content of the rock. Some high-temperature steady-state creep laws have been established however, and may be used as a first estimate of the exact continental-crust rheology. They correspond to a power-law creep behaviour, similar to that observed for olivine, with a stress exponent, n, of around 3.

Strength envelope

Using the hypotheses of Brace & Kohlstedt (1980), the minimum deviatoric stress required to extend the lithosphere at a given strain rate presents a variation with depth

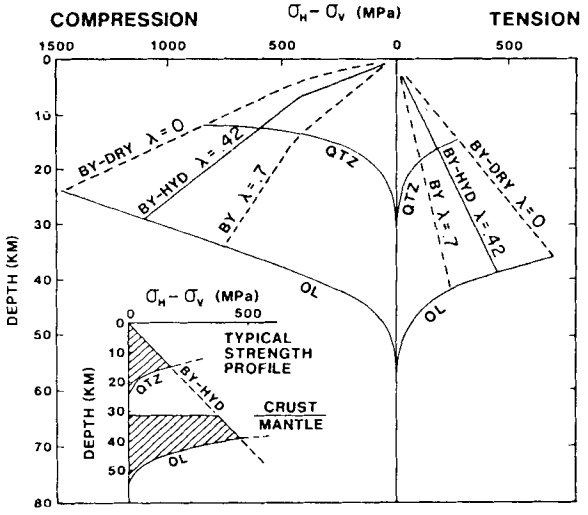

Figure 1. Deviatoric stress required to deform crust and upper mantle rocks at a given strain rate (here, $10^{-15}\,s^{-1}$) as a function of depth. Values of λ give pore-pressure level as a fraction of lithostatic pressure. Lines labelled BY are from Byerlee's law; lines labelled QTZ (quartz) and OL (olivine) are from a ductile-flow law. The geothermal gradient is $15°\,km^{-1}$. The inset shows a typical strength profile in tension for a continental lithosphere with a crustal thickness of 31.25 km (from Sawyer 1985).

like that illustrated in Fig. 1. Note that this curve is often interpreted incorrectly as a strength envelope curve; actually it does not represent an absolute strength and it is only valid for a given, uniform strain rate. In any case, it approximates the continental lithosphere using three or four layers of different mechanical behaviour and thickness: the upper crust is always in a brittle regime whereas the lower crust deforms by steady-state creep. For the conditions assumed in Fig. 1, the upper mantle, just below the Moho, undergoes brittle deformation but for other values of the parameters the whole mantle lithosphere flows. These parameters are essentially the crust thickness, the geotherm, the pore pressure and its variations with depth, and the strain rate.

This mechanical structure of the lithosphere suggests several points. In particular, it is worth noting that olivine is stronger than quartz at similar temperatures and pressures, although the magnitude of this discontinuity is expected to vary appreciably with temperature and strain rate. As a consequence, the Moho corresponds generally to an important increase in strength. In addition, the strong temperature-dependence of creep laws leads to a sharp decrease in strength with depth in the ductile layers (the lower crust and the lower part of the mantle lithosphere). In addition, in the brittle layers, the strength increases progressively with depth and reaches a maximum at the brittle–ductile transition. This probably overestimates the stress at this rheological interface but, in the absence of more precise details about this transition, it is the simplest way to localize it.

Stability of continental lithosphere extension

Having the above model in mind, we would like to address the following questions: Can the lithosphere exhibit a necking instability when it is submitted to tension? And, if so, how does the deformation proceed in the constricted

part before rupture? Only partial answers to these questions may be found in previous works, because on the one hand theoretical study on necking instabilities is still incomplete (Jalinier 1981), and on the other hand it has been developed for situations that have very little in common with those of the lithosphere.

Several criteria have been proposed to specify the conditions in which a sample submitted to uniaxial stress σ can extend stably. Each produces slightly different conclusions in the most general case. However, for any of these criteria, a material characterized by a constitutive law of the type:

$$\dot{\varepsilon} = \alpha\sigma^n \tag{1}$$

(where $\dot{\varepsilon}$ is the strain rate and α is a constant) is unstable with respect to tension if $n \geq 3$ (Rossard 1966; Hart, Campbell 1967); the rate at which the instability grows increases with the stress exponent n.

To examine what consequences the preceding conditions have for stretching of the lithosphere, let us consider the different rheologies that we have retained to describe it. For the ductile lower crust and mantle, we have adopted a power-law behaviour with $n = 3$; extension of such layers should then be unstable but the instability is expected to grow slowly. The perfectly plastic rheology that we have introduced to describe the brittle layers corresponds to the limit case $n \to \infty$; according to the above criteria, these layers are expected to be very unstable with respect to tension and, thus, to play an important role in the present discussion. It is important to emphasize that this property results from a description of the brittle layers' rheology that is not straightforward, as already mentioned.

Continental lithosphere appears therefore to be made up of several layers that are unstable with respect to tension. Regardless of the rheological uncertainties themselves, this conclusion does not provide much information about the behaviour of the lithosphere as a whole. If a layer starts to neck, for example, the adjacent layers will respond by swelling and the total lithospheric deformation will not be obvious. Furthermore, the lithosphere is not submitted to uniaxial stress and, in particular, it is subject to the gravity-field so that the gravity contrasts at the interfaces will act to stabilize or destabilize the flow.

Taking this complexity into account, there seems to be no way other than by a direct determination to make evident any eventual instability. We already mentioned that necking generally begins in a zone where the sample presents a 'defect'. In our case, this defect will be a small variation of thickness of the layers and we shall examine the evolution of these variations when the lithosphere is stretched.

MODEL OF INHOMOGENEOUS EXTENSION OF THE LITHOSPHERE

We consider a model of lithosphere of infinite horizontal extent, consisting of three or four layers. The various interfaces, instead of being planar, exhibit an initial topography. The purpose of the following study is to examine whether these disturbances can be amplified through stretching, leading to enhanced thinning of certain layers or zones. To this end, the stresses and velocity of deformation must be determined in the extending lithosphere. The method we used to compute them has been proposed by Smith (1977) and assumes that the amplitudes of the disturbances remain small with respect to the layer thicknesses, so that the modification they introduce may be regarded as perturbations from a basic state of uniform extension.

Basic state. Rheological approximations

Let us suppose for the moment that the lithosphere consists of parallel horizontal layers. We asume that this structure undergoes plane strain, in the plane $(0, x, z)$, and deforms in a pure shear strain field. As a consequence, only the two terms $\dot{\varepsilon}_{xx}$ and $\dot{\varepsilon}_{zz}$ of the strain rate tensor are different from zero. Incompressibility of the material requires furthermore that:

$$\dot{\varepsilon}_{xx} + \dot{\varepsilon}_{zz} = 0. \tag{2}$$

The ductile layers are described by the constitutive laws of fluid mechanics, i.e.

$$\sigma_{ij} = 2\eta\dot{\varepsilon}_{ij} - p\delta_{ij}, \tag{3}$$

where σ_{ij} is the stress tensor, $\dot{\varepsilon}_{ij}$ the strain rate tensor, p is the hydrostatic stress; viscosity η is given by:

$$2\eta = B^{-1}\exp(Q/RT)J_2^{(1-n)/2}, \tag{4}$$

where the constants B, Q and n are material properties and $J_2 = \frac{1}{4}[(\sigma_{xx} - \sigma_{zz})^2] + \sigma_{xz}^2$ is the second invariant of the deviatoric stress.

In the following sections, all the physical quantities relative to the basic state will be denoted by an overbar. For a pure shear strain field, it results from (2) and (3) that:

$$\bar{\sigma}_{xx} - \bar{\sigma}_{zz} = 4\bar{\eta}\dot{\bar{\varepsilon}}_{xx} \tag{5}$$

$$\bar{\sigma}_{xz} = 0 \tag{6}$$

and consequently:

$$\bar{J}_2 = 4\bar{\eta}^2\dot{\bar{\varepsilon}}_{xx}^2. \tag{7}$$

Then

$$\bar{\eta} = \tfrac{1}{2}(\dot{\bar{\varepsilon}}_{xx})^{(1-n)/n}B^{-1/n}\exp(Q/nRT), \tag{8}$$

which may be written in the form:

$$\bar{\eta} = K\exp(Q/nRT), \tag{9}$$

where K is a constant for a given layer. This viscosity law couples the mechanical and thermal problems, thus requiring the use of a numerical method to solve the Navier–Stokes equation. However, an analytic solution can be obtained without neglecting the very rapid decrease of viscosity with increasing depth and temperature by assuming, as suggested by Fletcher & Hallet (1983), that:

$$\bar{\eta}(z) = \eta_0\exp(\gamma z), \tag{10}$$

where η_0 and γ are constants. We shall detail in a following section how they are chosen for each ductile layer in the lithosphere.

We have already mentioned that brittle layers are approximated as ideally plastic materials. To describe their behaviour beyond the yield stress, it is equivalent to consider them as power-law fluids with a large stress

exponent (Fletcher & Hallet 1983), since for such a fluid, as for a perfect plastic material obeying Von Mises criterion, the second invariant J_2 is almost unchanged by a small modification of the strain tensor (Bassi 1986). With these assumptions, relations (3) to (7) hold in the brittle layers. Moreover, the Von Mises criterion requires that:

$$J_2 = \tau_y^2 \tag{11}$$

if τ_y is the yield stress. The effective viscosity is thus related to τ_y by:

$$\tau_y = 2\bar{\eta}\dot{\bar{\varepsilon}}_{xx} \tag{12}$$

and should be a linear function of depth according to Byerlee's law. We shall neglect this variation of the yield stress with depth and consider $\bar{\eta}$ to be a constant, as the Navier–Stokes equation can be solved analytically in this case. Of course, this approximation and the preceding ones could be avoided by the use of numerical techniques which would allow a more precise incorporation of the exact depth-dependent rheology in the model. However, we preferred the analytic approach which, despite its simplicity, is often sufficient in a first-order analysis and is a more flexible way to investigate the influence of the various parameters.

Perturbation of the basic state: linearization of the constitutive relations

Let us suppose now that the planar geometry of the interfaces is altered and presents small disturbances along the x axis. The strain rate and stress tensors, as well as the velocity field, will of course be modified, but the modifications can be treated as perturbations of the basic state if the interface amplitudes remain small with respect to the layer thicknesses. Therefore, we can write all the physical quantities of the problem as the sum of a basic state value and a perturbation (denoted with a tilde) (Smith 1977).

The perturbing strain rate tensor $\dot{\tilde{\varepsilon}}_{ij}$ cannot be estimated independently of $\dot{\bar{\varepsilon}}_{ij}$ since the constitutive laws (3) and (4) are not linear. However, to the first order in $\dot{\tilde{\varepsilon}}_{ij}/\dot{\bar{\varepsilon}}_{ij}$ it may be shown that (Smith 1977; Fletcher & Hallet 1983):

$$\begin{cases} \tilde{\sigma}_{xz} = 2\bar{\eta}\dot{\tilde{\varepsilon}}_{xz} \\ \tilde{\sigma}_{xx} = \dfrac{2\bar{\eta}}{n}\dot{\tilde{\varepsilon}}_{xx} - \tilde{p} \\ \tilde{\sigma}_{zz} = \dfrac{2\bar{\eta}}{n}\dot{\tilde{\varepsilon}}_{zz} - \tilde{p}. \end{cases} \tag{14}$$

It is interesting to note that, compared to the basic state, the effective viscosity is divided by a factor, n, for normal strain, but remains unchanged for shear strain. This result will have important consequences in the brittle layers where n is supposed to be very large.

Boundary conditions

A solution for the perturbing flow is found by requiring that the perturbing stresses and strain rates satisfy the equilibrium and incompressibility equations, i.e.

$$\nabla\tilde{\boldsymbol{\sigma}} = 0 \tag{15}$$

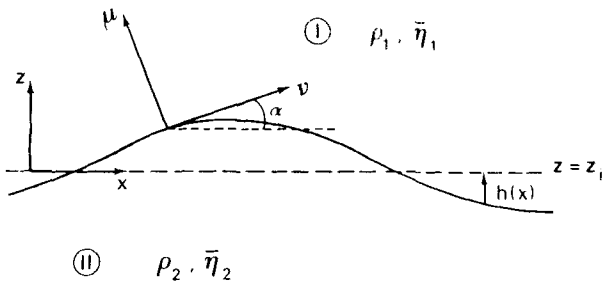

Figure 2. Geometry of the interface between layers I and II. Velocities and stresses are continuous through the real interface located on $z = z_i + h$.

and

$$\dot{\tilde{\varepsilon}}_{xx} + \dot{\tilde{\varepsilon}}_{zz} = 0. \tag{16}$$

The approximations introduced in the preceding sections allow these equations to be solved analytically in each layer of the lithosphere. The integration coefficients are determined by writing the boundary conditions at the interfaces. Let us consider one of these, separating a layer I of density ρ_1 and viscosity $\bar{\eta}_1$, from a layer II of density ρ_2 and viscosity $\bar{\eta}_2$, and presenting a disturbance $h(x)$ with respect to a mean position z_i (Fig. 2). The boundary conditions require that the velocities u and w, horizontal and vertical respectively, and the stress components σ_{xz} and σ_{zz} are continuous on the true interface, i.e. on $z = z_i + h$. When h is small, these conditions may be expanded to first-order with respect to h, and written on the mean interface $z = z_i$ where they become (Smith 1977)

$$\tilde{w}^I(x, z_i) - \tilde{w}^{II}(x, z_i) = 0 \tag{17}$$

$$\tilde{u}^I(x, z_i) - \tilde{u}^{II}(x, z_i) = 0 \tag{18}$$

$$\tilde{\sigma}^I_{xz}(x, z_i) - \tilde{\sigma}^{II}_{xz}(x, z_i) = 4\dot{\bar{\varepsilon}}_{xx}(dh/dx)[\bar{\eta}_1(z_i) - \bar{\eta}_2(z_i)] \tag{19}$$

$$\tilde{\sigma}^I_{zz}(x, z_i) - \tilde{\sigma}^{II}_{zz}(x, z_i) = (\rho_2 - \rho_1)gh(x). \tag{20}$$

These expressions hold for any perturbation $h(x)$ and are linear in h. Therefore, the problem reduces to the treatment of each Fourier component of the topography and the associated flow. The advantage of this spectral analysis lies in the particularly simple determination of velocities and stresses for a sinusoidal topography; this determination is further developed in Appendix A.

Evolution of the amplitude of the interfaces through time

Substitution of the general expressions of velocities and stresses into the boundary conditions (17) to (20) yields a set of linear equations (see Appendix A) which may be written in the form:

$$m\mathbf{C} = \mathbf{R}, \tag{21}$$

where, if m is the number of deformable interfaces, M is a $4m$-order square matrix, $\mathbf{C}$ is the integration coefficients vector, $\mathbf{R}$ is a $4m$-order vector corresponding to the right-hand side of conditions (17) to (20).

Let h_{i0} be the amplitude of the sinusoidal undulation of the interface i, and $\mathbf{H}$ the vector of generic term h_{i0}. The following method, proposed by Ricard & Froidevaux

(1986), allows us to compute the evolution of **H** through time.

Considering λ, the wave number, as independent of time (since we are limited to the initial stages of the deformation), the growth of $h_i(x)$ is $h_{i0}\cos\lambda x$; its magnitude is equal to the total vertical velocity at the interface, i.e.

$$\tilde{w}(0, z_i) - \dot{\bar{\varepsilon}}_{xx} h_i(x).$$

Therefore, the vector **H** satisfies:

$$d\mathbf{H}/dt = \mathbf{W} - \dot{\bar{\varepsilon}}_{xx}\mathbf{H},$$

where **W** is the vector of generic term $w_i = \tilde{w}(0, z_i)$. **W** is a linear function of **C**, let us say:

$$\mathbf{W} = Q\mathbf{C}$$

or

$$\mathbf{W} = QM^{-1}\mathbf{R}$$

where Q is a $m \times (4m)$-order matrix. In addition, **R** is a linear function of **H** since the right-hand side of boundary conditions (17) to (20) is proportional to h if h is a sine function; then

$$\mathbf{R} = P\mathbf{H},$$

where P is a $(4m) \times m$ matrix. Finally,

$$d\mathbf{H}/dt = (QM^{-1}P - \dot{\bar{\varepsilon}}_{xx} I)\mathbf{H}. \tag{22}$$

The second term in the right-hand side of this relation results from uniform stretching and does not correspond to any amplification or attenuation of the topography with respect to the layer thicknesses. The contribution of the perturbing flow is obtained by solving the reduced system:

$$d\mathbf{H}/dt = QM^{-1}P\mathbf{H},$$

which is a first-order differential system with constant coefficients. More precisely, the matrix $QM^{-1}P$ depends on the mechanical properties and thickness of the layers, and on the wave number λ; both may be considered as constant in the early stages of the deformation.

The standard way of solving this system consists in computing the eigenvalues $q_i\dot{\bar{\varepsilon}}_{xx}$ of the matrix $QM^{-1}P$ and the associated eigenvectors $\mathbf{V}_i$, which are independent of time. The vector **H** at time t may then be written in the form:

$$\mathbf{H}(t) = \sum_{i=1}^{m} \exp(q_i\dot{\bar{\varepsilon}}_{xx}t)a_{i0}\mathbf{V}_i, \tag{23}$$

where the constants $a_{i0}\,(i = 1, m)$ are determined from **H**(0).

The eigenvectors $\mathbf{V}_i$ are the natural modes of deformation of the system. When **H**(0) is equal to one of these vectors, say $\mathbf{V}_i$, the vector **H**(t) remains proportional to **H**(0), with the amplitude of the interfaces being amplified or attenuated through time according to the sign of the eigenvalue $q_i\dot{\bar{\varepsilon}}_{xx}$.

It is important to keep in mind, however, that relation (23) is only valid as long as the $h_i\,(i = 1, m)$ remain small with respect to the layer thicknesses.

From equations (22) and (23), it appears that an instability of the deformation, that is to say a growth of the topographies, can only be observed if at least one of the eigenvalues of the problem is positive and greater than 1. The largest eigenvalue (we shall label it q) represents the maximum of amplification, and an initial distribution of amplitudes corresponding to its eigenvector is the most favourable to the development of the instability. For this reason, we shall present our results in the form of a curve showing the variation of q as a function of wave number λ.

PARAMETER VALUES

In most of the previous works (e.g. Fletcher & Hallet 1983; Zuber *et al.* 1986), the structure of interest was underlain by an infinite substrate. We noticed, however, that these models lead to infinite velocities in the limiting case $\lambda = 0$. Such divergence problems may be avoided by using finite-thickness layers (Bassi 1986). For this reason, we assume that the velocities $\tilde{u}$ and $\tilde{w}$ vanish at the base of the deepest layer, which is taken to be the asthenosphere. Theoretically, this layer has the same mechanical behaviour as the mantle lithosphere and constitutive relations (3) and (4) should hold in it. However, the linearized equations (14) explicitly suppose that the layer is submitted to uniform extension. They cannot apply to the asthenosphere if it is not stretched along with the lithosphere. To avoid any further assumption about the basic deformation of the asthenosphere, we shall describe it as a Newtonian fluid.

Even in the simplified approach of Brace & Kohlstedt (1980), the model of lithospheric rheology depends on a number of parameters which are poorly constrained by the data; we recalled them in the preceding section. However, previous work on lithospheric strength has demonstrated that lithosphere deformation is critically controlled by its thermal structure (Kusznir & Park 1984). Hence, we shall focus on the influence of the geotherm on the modelling of lithospheric rheology, taking the other parameters as essentially fixed. In particular, the continental crust is assumed to be 35 km thick and its density is taken as $2.8\,\mathrm{g\,cm^{-3}}$. When it is ductile, it is characterized by a quartz creep law, let us say (Christie *et al.*, cited by Vink *et al.* 1984):

$$\dot{\bar{\varepsilon}}_{xx} = 2.4 \times 10^{-7}(\bar{\sigma}_{xx} - \bar{\sigma}_{zz})^3 \exp\left[-\frac{149 \times 10^3}{RT}\right] \tag{24}$$

if $\bar{\sigma}_{xx} - \bar{\sigma}_{zz}$ is expressed in MPa.

In the mantle, we adopt the flow law proposed by Goetze & Evans (1979) for dislocation creep of olivine, which has been confirmed by more recent experiments (Kirby 1983):

$$\dot{\bar{\varepsilon}}_{xx} = 7 \times 10^4(\bar{\sigma}_{xx} - \bar{\sigma}_{zz})^3 \exp\left[-\frac{520 \times 10^3}{RT}\right]. \tag{25}$$

The mineralogical composition of the asthenosphere does not fundamentally differ from that of the mantle lithosphere, as already mentioned. However, the former is, on average, warmer than the latter so that its mean density is less. As a consequence, we took a density of $3.3\,\mathrm{g\,cm^{-3}}$ for the mantle lithosphere and $3.25\,\mathrm{g\,cm^{-3}}$ for the asthenosphere. The base of the lithosphere is defined by the 1300 °C isotherm, following McKenzie (1978) among others.

To construct the strength envelope of Brace & Kohlstedt (1980), we assume furthermore that there is no fluid

pore-pressure (a condition which eventually exaggerates the total lithospheric strength) and that the mean rate of deformation $\dot{\varepsilon}_{xx}$ is 10^{-15} or $10^{-16}\,s^{-1}$, these values being considered as typical of lithospheric-deformation velocity.

The various geotherms we investigated were constructed following a model proposed by Morgan & Sass (1984). The radiogenic heat production is supposed to be an exponential function of depth in the continental crust (with a constant thermal conductivity $k = 2.5\,W\,m^{-1}\,K^{-1}$) and to vanish in the mantle (where $k = 3.4\,W\,m^{-1}\,K^{-1}$). These models essentially depend on two parameters H_s and q_m, which are respectively the radiogenic heat production at the surface and the heat flow at the base of the crust. They are related to the surface heat flow q_s by the relation:

$$q_s = q_m + H_s b,$$

where b is the heat-production decay length, taken as 10 km following usual estimations (Morgan & Sass 1984; Turçotte & Schubert 1982). According to Morgan & Sass (1984), q_m comprises between $30\,mW\,m^{-2}$ and $50\,mW\,m^{2}$ whereas H_s, which strongly depends on the thermal history of the lithosphere, can vary between 0 and $6\,\mu W\,m^{-3}$. Of the numerous models of a geotherm that these limits allow us to construct we retained a few corresponding to a surface heat-flow greater than or equal to $50\,mW\,m^{-2}$. It is improbable, as we mentioned before, that continental lithosphere may undergo significant deformation through geological time if its surface heat-flow is less than this value.

The strength stratification of the lithosphere that results from the above model is summarized in Table 1. The total lithospheric thickness depends primarily on the value of q_m and varies between 67 ($q_m = 50\,mW\,m^{-2}$, $H_s = 4\,\mu W\,m^{-3}$) and 127 km ($q_m = 30\,mW\,m^{-2}$, $H_s = 2\,\mu W\,m^{-3}$). The thickness of the brittle upper crust is of the order of 10 km; this is consistent with observations of seismicity under continents as the depth of continental intraplate earthquakes is generally 15 km or less. The surface-layer thickness increases as expected with decreasing surface heat-flow; it also increases with the rate of deformation, in agreement with experimental results of rock mechanics (Jaeger & Cook 1976). The same remarks apply to the mantle brittle layer when it exists, which essentially depends on the value of q_m.

In addition to the various thicknesses, the discussion of lithospheric extension stability depends on a number of dimensionless parameters which are summarized in Fig. 3 and Table 2. Note that the stress exponent is taken as $n = 1000$ in the upper crust and brittle mantle in order to approximate a perfectly plastic rheology (Fletcher & Hallet 1983). Let us summarize how the values of the other parameters are determined for each lithospheric model.

If h_c is the crust thickness, $\gamma_c h_c$ and $\gamma_m h_c$ are the inverses of viscosity decay lengths, respectively, in the lower crust and in the ductile mantle lithosphere. To estimate their value, Fletcher & Hallet (1983) constrain the exact viscosity curve (equation 4) and the approximate one (equation 10) to give the same viscosity and the same rate of change with depth at the top of the layer. However, this method leads to a very rapid decrease of viscosity with depth and to anomalously low values at the base of the layer. For this reason, we found it more appropriate to constrain the approximate viscosity law to take the exact values at the base and the top of the considered layer. These are easily computed using equations (4) and (7).

$\Delta\eta_q$, $\Delta\eta_M$ and $\Delta\eta_0$ are the ratios of strengths respectively at the crust brittle-ductile transition, at the Moho, and at the eventual brittle-ductile transition of the mantle. Except in some specified cases, the viscosity is continuous through the base of the lithosphere which is essentially a thermal interface. As we have taken into account the decrease of viscosity with increasing temperature in the lithosphere, there is no particular argument to introduce a discontinuity at the lithosphere–asthenosphere transition.

Estimation of the above ratios requires the definition of the brittle–layer equivalent viscosity which, as stated before, is a constant related to the yield strength by equation (12). If the linear increase of τ_y with depth has to be approximated by a constant, it seems appropriate to choose the average value of τ_y as typical of the layer strength. The determination is then straightforward since Byerlee's law allows computation of $(\bar{\sigma}_{xx} - \bar{\sigma}_{zz}) = 2\tau_y$ as a function of depth (see Appendix B).

Finally, gravity is involved through parameters S_s, S_M and S_L which measure the intensity of gravitational stresses compared to extensional stresses (Ricard & Froidevaux 1986).

Table 1. Influence of the geotherm and the rate of deformation on the thickness of lithospheric layers. q_s is the surface heat flow, q_m and H_s are defined in the text; t_L, t_{bc}, t_{dc}, t_{bm} and t_{dm} are the respective thicknesses of the lithosphere, of the brittle upper crust, of the ductile lower crust, of the brittle mantle and the ductile mantle lithosphere. L_d is the dominant wavelength of Figs 4 and 5.

q_s ($mW\,m^{-2}$)	q_m ($mW\,m^{-2}$)	H_s ($\mu W\,m^{-3}$)	$\dot{\varepsilon}_{xx}$ (s^{-1})	t_L (km)	t_{bc} (km)	t_{dc} (km)	t_{bm} (km)	t_{dm} (km)	L_d (km)
50	30	2	10^{-16}	127	12	23	16	76	
50	30	2	10^{-15}	127	14	21	20	72	61
60	40	2	10^{-16}	93	10	25	2	56	
60	40	2	10^{-15}	93	12	23	4	54	48
70	30	4	10^{-16}	120	10	25	9	76	
70	30	4	10^{-15}	120	11	24	13	72	61
70	50	2	10^{-16}	72	9	26	0	37	
70	50	2	10^{-15}	72	10	25	0	37	41
80	40	4	10^{-16}	87	8	27	0	52	48
80	40	4	10^{-15}	87	10	25	0	52	48
90	50	4	10^{-16}	67	7	28	0	32	44
90	50	4	10^{-15}	67	8	27	0	32	44
100	40	6	10^{-16}	81	7	28	0	46	
100	40	6	10^{-15}	81	8	27	0	46	51

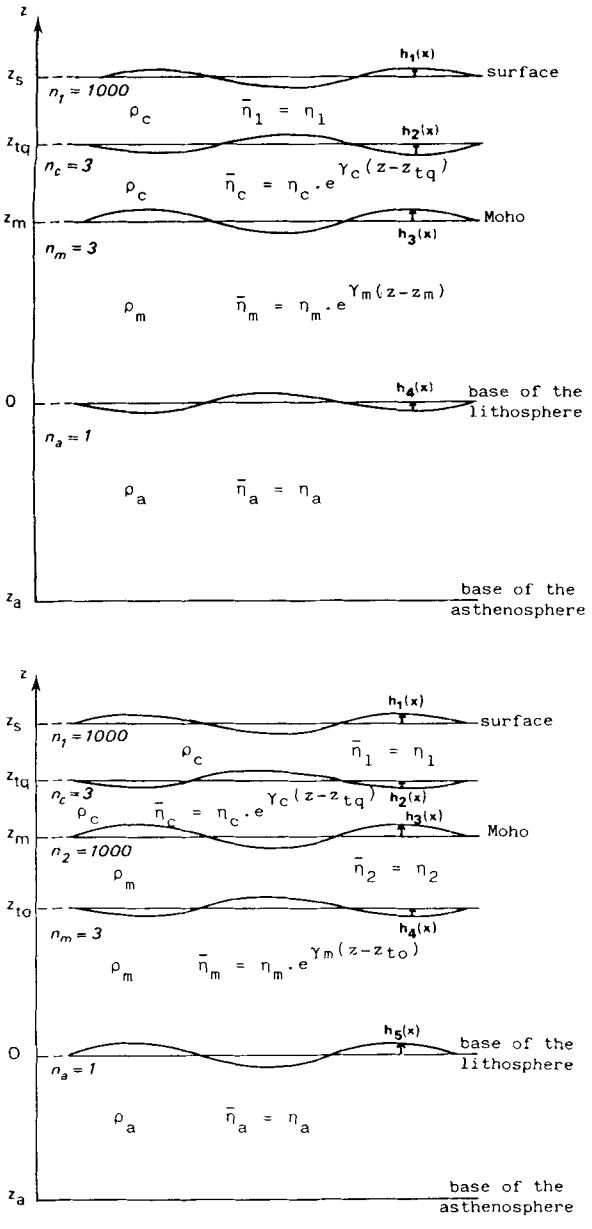

Figure 3. Model of three-layer (A) and four-layer (B) lithosphere under extension. Discontinuities of density or viscosity occur at each interface except, for the density, at the brittle–ductile transition and, for the viscosity, at the lithosphere–asthenosphere boundary. No velocity is assumed at the base of the asthenosphere.

The resulting parameter values are reported in Table 3 for each lithospheric model. Let us remark, first, that $\Delta\eta_q$ and $\Delta\eta_0$ are always greater than 1; this means that the brittle layers are, on average, easier to deform than the immediately underlying medium. This particular configuration will have important consequences for the results, as we shall see below.

Previous discussions about stability of non-Newtonian fluids with respect to tension (Smith 1977; Fletcher & Hallet 1983) have led to the conclusion that large values of the stress exponent n are required for the development of an instability. Furthermore, the growth rate factor q, which measures the rate of increase of the topography, increases with n. This is in good agreement with the general criteria of

Table 2. Dimensionless parameters required for the determination of the perturbing flow (h_c is the crust thickness; the other notations are defined in Fig. 3).

(*a*) *Three-layer lithosphere:*

$k = \lambda h_c$

n_1, n_c, n_m

z_s, z_{tq}, z_m, z_a

$\gamma_c h_c, \gamma_m h_c$

$\Delta\eta_q = \dfrac{\eta_c}{\eta_1}$ and $\Delta\eta_M = \dfrac{\eta_m}{\bar{\eta}_c(z_m)}$

$S_s = \dfrac{\rho_c g h_c}{2\tau_{y1}} = \dfrac{\rho_c g h_c}{4\dot{\bar{\varepsilon}}_{xx}\eta_1}$, $S_M = S_s \dfrac{\rho_m - \rho_c}{\rho_c}$ and $L_L = \dfrac{\rho_a - \rho_m}{\rho_c}$

(*b*) *Four-layer lithosphere:*

In addition to the above parameters, it is necessary to define:

n_2

z_{t0}

$\Delta\eta_0 = \eta_m/\eta_2$

stability we have mentioned above and confirms that the brittle layers, the upper crust and in some cases the upper part of the mantle, will play an important role in the discussion.

Fletcher & Hallet (1983) have considered the case of a strong surface layer of uniform strength τ_y overlying a ductile substrate with exponentially varying strength. By hypothesis, there is no discontinuity of density or strength between the two layers. Introducing the parameter

$$S = \frac{\rho g h}{2\tau_y},$$

where h is the surface-layer thickness, they have shown that, with a favourable value of the stress exponent of the surface layer,

$$\gamma h > S, \tag{27}$$

where γh is the inverse of the viscosity decay length, is a necessary condition for an unstable growth of the surface topography. As S describes the effect of gravity which is stabilizing if the density increases with depth, this parameter should be small enough to allow the development of an instability. On the contrary, γh is related to the viscosity contrast between the unstable layer and the surrounding medium, and ought to be as great as possible. When these two parameters are chosen according to (27), the mechanical effect dominates the gravity effect.

How does this condition apply in our case? As far as the surface layer is concerned, we notice that S_s is comparable to $\gamma_c h_c$, or even greater; according to relation (27), a growth of topography is unlikely in this context.

The mantle brittle layer is surrounded by two different media and the application of the above condition is not straightforward. However, since there is strong increase of viscosity at the Moho (Fig. 1), it is probable that the lower crust will have a negligible effect on the behaviour of the mantle. Let us therefore compare $\gamma_m h_c$ and:

$$S'_M = \frac{(\rho_m - \rho_c) g h_c}{2\tau_{y2}}$$

Table 3. Parameter values for the models of lithosphere of Table 1.

q_m (mW m^{-2})	H_s (μW m^{-3})	$\dot{\varepsilon}_{xx}$ (s^{-1})	$\gamma_c h_c$	$\gamma_m h_c$	S_s	S_M	S_L	$\Delta\eta_q$	$\Delta\eta_M$	$\Delta\eta_0$
30	2	10^{-16}	7.4	4.5	7.3	1.3	−0.13	1.8	253	2.5
30	2	10^{-15}	6.9	4.4	6.2	1.1	−0.11	1.7	124	2.1
40	2	10^{-16}	8.1	5.9	8.7	1.6	−0.16	1.6	806	1.5
40	2	10^{-15}	7.5	5.7	7.3	1.3	−0.13	1.2	396	1.8
30	4	10^{-16}	7.0	4.5	8.7	1.6	−0.16	1.3	458	2.2
30	4	10^{-15}	6.7	4.3	7.9	1.4	−0.14	1.7	219	2.0
50	2	10^{-16}	8.4	6.5	9.7	1.7	−0.17	1.2	240	—
50	2	10^{-15}	8.0	6.5	8.7	1.6	−0.16	1.4	240	—
40	4	10^{-16}	8.0	5.6	10.9	1.9	−0.19	1.9	680	—
40	4	10^{-15}	7.2	5.6	8.7	1.6	−0.16	1.1	680	—
50	4	10^{-16}	8.5	6.1	12.5	2.2	−0.22	1.9	99	—
50	4	10^{-15}	8.0	6.1	10.9	1.9	−0.19	1.9	99	—
40	6	10^{-16}	7.7	5.2	12.5	2.2	−0.22	1.4	246	—
40	6	10^{-15}	7.2	5.2	10.9	1.9	−0.19	1.5	246	—

where τ_{y2} refers to the strength of the mantle brittle layer. As $\tau_{y2} > \tau_{y1}$, $S'_M < S_M$. Then, it appears from Table 3 that $\gamma_m h_c > S'_M$.

The appropriate coefficients satisfy relation (27) so that it would be possible to observe a mechanical instability if $\Delta\eta_0$ was 1 or less, as assumed in Fletcher & Hallet (1983). Since this condition is not fulfilled, their analysis cannot be used to speculate about the growth of a stretching instability in the mantle brittle layer.

RESULTS

For all the situations we have considered, i.e. for the lithospheric models of Tables 1 and 3 and a mean rate of deformation of 10^{-15} s^{-1}, the evolution of the growth rate factor q as a function of dimensionless wave number $k = \lambda h_c$ is similar (Figs 4 and 5); q increases rapidly with k, reaches a maximum and then slowly decreases. The maximum value comprises between 14 and 20 and the corresponding wavelength L is of the order of 50 km; the small variations of L seem well correlated with the lithosphere thickness or with its mantle-part thickness (Table 1).

Reducing the rate of deformation $\dot{\varepsilon}_{xx}$ does not modify the form of the curve or the dominant wavelength (Fig. 6) but the associated maximum increases: for a lithosphere with a surface heat-flow of 80 mW m^{-2}, the maximum reaches 33 when $\dot{\varepsilon}_{xx} = 10^{-16}$ s^{-1}, instead of 15 for $\dot{\varepsilon}_{xx} = 10^{-15}$ s^{-1}. This effect of the rate of deformation is rather surprising. As noted by Ricard & Froidevaux (1986), the interface relief is the result of two competing factors: gravity, which generally tends to damp the topography, and stretching instabilities which tend to enhance it. As a consequence, when the deformation is driven by large deviatoric stresses, i.e. large values of $\dot{\varepsilon}_{xx}$ (equation 5), the effect of gravity should be negligible and the growth-rate factor should increase. This is opposite to our results and suggests that the instability we observe does not come from stretching.

The mode of deformation associated with the eigenvalue q (Figs 4 and 5), independently of wave number and lithospheric model, corresponds to a situation where all the interfaces, except the lithosphere–asthenosphere boundary, remain planar. Now, this interface is the only one which is characterized by an inversion of density and therefore where gravity has a destabilizing effect. One may wonder whether the instability for which we have evidence was not simply gravitational in origin. This may easily be verified by changing the asthenosphere density; if this quantity is 3.35 rather than 3.25 g cm^{-3}, only the sign of S_L is modified. With this new density value, and for a three-layer lithosphere, the growth rate factor is negative for all the wave numbers of interest (Fig. 7). This result is not too

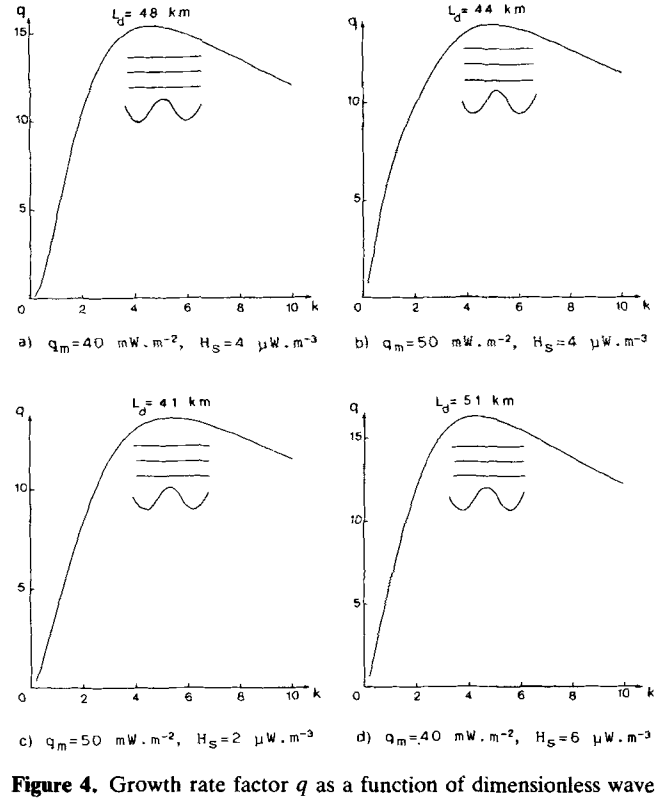

Figure 4. Growth rate factor q as a function of dimensionless wave number $k = \lambda h_c$ for models of three-layer lithosphere. Each model corresponds to a given geotherm and is characterized by the value of q_m, the heat flow at the base of the crust, and H_s the radiogenic heat production at the surface. The mean rate of extension $\dot{\varepsilon}_{xx}$ is 10^{-15} s^{-1} L_d refers to the wavelength for which q is maximum. Schematically represented on each curve is the mode of deformation associated with q which is approximately independent of k.

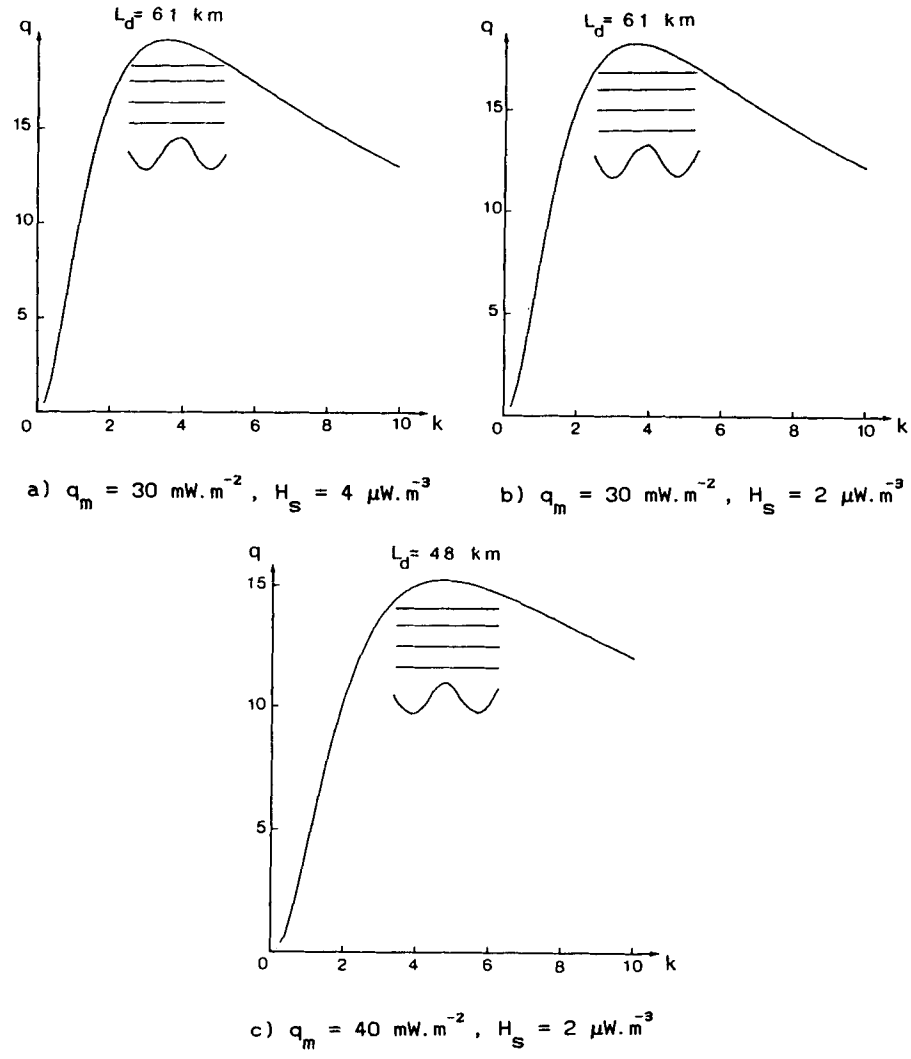

Figure 5. Same plot as in Fig. 4 but for models of lithosphere consisting of four layers. Note that all the situations considered in this figure and the preceding one give very similar results.

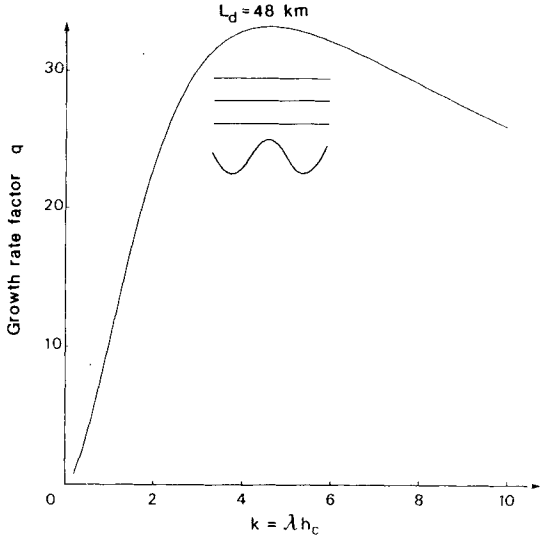

Figure 6. Effect of the rate of extension on the growth-rate factor. This curve, constructed for $\dot{\varepsilon}_{xx} = 10^{-16}\,s^{-1}$, should be compared with Fig. 4(a) which corresponds to the same model of the lithosphere. Neither L_d nor the deformation pattern is modified, but the maximum value of q is increased.

surprising since the only unstable layer, the upper crust, is placed in conditions which are not favourable to the growth of a stretching instability, as noted earlier.

When the mantle lithosphere is not entirely ductile (Fig. 8), q is positive in a narrow range of wave numbers; these positive values correspond to boudinage or buckling of the brittle part of the mantle. However, the maximum value of q is always less than 1 so that, if uniform stretching is taken into account, the topography will not be amplified but rather attenuated through time (equation 22). In this latter case also, the results are consistent with our previous comments: even if $\gamma_m h_c$ is greater than S'_M, the increase of equivalent viscosity at the brittle–ductile transition in the mantle inhibits the development of an instability.

We can therefore conclude that the results obtained for an asthenospheric density of 3.25 g cm^{-3} simply represent the gravitational instability of the asthenosphere with respect to the cooler lithosphere. The influence of the rate of deformation $\dot{\varepsilon}_{xx}$ is easy to interpret in this context: whereas in the case of mechanical instabilities, stretching is the driving mechanism and gravity the limiting one, the situation is reversed here: if the deformation is driven by large extensional stresses, they may inhibit the gravitational deformation of the lithosphere–asthenosphere boundary.

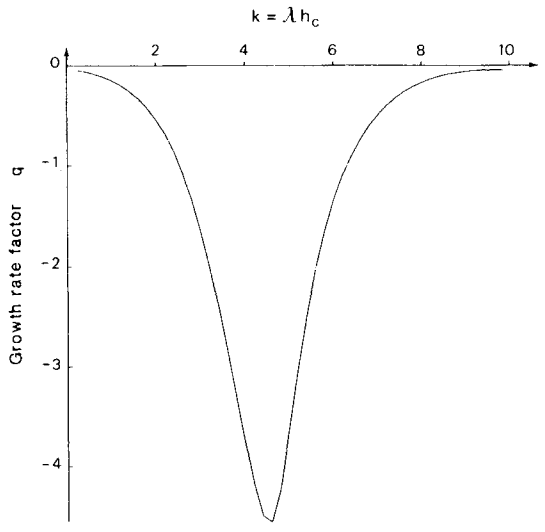

Figure 7. Effect of the density contrast at the lithosphere–asthenosphere boundary on the curve $q(k)$. The parameter values are those of Fig. 4(a) ($q_m = 40\,\mathrm{mW\,m^{-2}}$, $H_s = 4\,\mu\mathrm{W\,m^{-3}}$, $\dot{\varepsilon}_{xx} = 10^{-15}\,\mathrm{s^{-1}}$) except that the asthenosphere density is 3.35 instead of $3.25\,\mathrm{g\,cm^{-3}}$. Note that q is never positive in the wave number range under consideration, i.e. for wavelengths greater than 20 km.

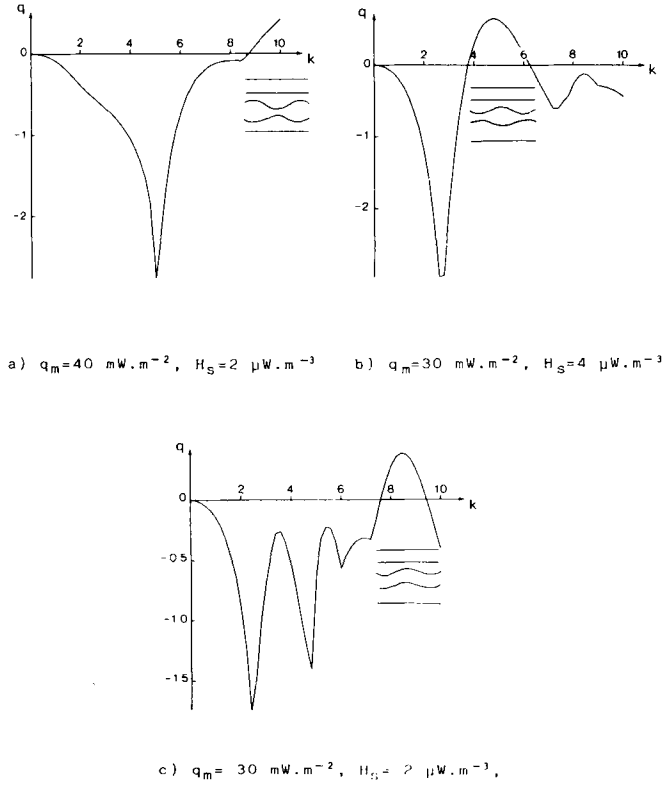

Figure 8. Same change of asthenosphere density as in Fig. 7, but for the models of lithosphere of Fig. 5. The growth-rate factor is positive in a restricted range of wave numbers (case b and c) and corresponds to buckling or boudinage of the brittle layer of the mantle; but q is always less than 1 so that no amplification of initial disturbances will be observed if uniform extension is taken in account.

DISCUSSION

According to the above model, and with parameter values which are closely related to the description of lithospheric rheology proposed by Brace & Kohlstedt (1980), this structure is stable with respect to necking and presents a gravitational instability if the asthenosphere is less dense than the overlying lithosphere. This conclusion disagrees with those of Ricard & Froidevaux (1986) and Zuber *et al.* (1986). It is interesting to establish whether some parameters, more than others, are responsible for this discrepancy.

Figure 9 corresponds to a typical set of parameter values used by Ricard & Froidevaux (1986). Their model consists of three constant viscosity layers (Fig. 9, upper part), chosen in such a way that:

$$\Delta\eta_q = 0.01$$

$$\Delta\eta_M = 100$$

$$\Delta\eta_a = 0.01.$$

These values rest on the assumption that the lithosphere consists of a strong upper crust and upper mantle, separated by a weak lower crust, and overlying a weak asthenosphere. Such a structure presents in the wave-number range of interest a well-defined instability (Fig. 9, lower part). The plot of growth-rate factor exhibits three distinct peaks corresponding respectively to 270, 47 and 21 km wavelengths. The first is associated with a boudinage-like

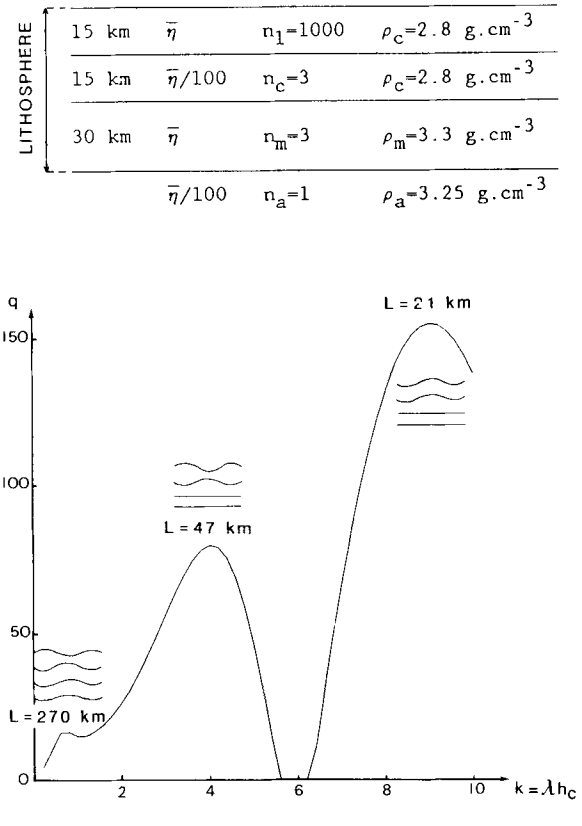

Figure 9. Model of lithosphere with constant-viscosity layers which is highly unstable with respect to tension. Parameter values are very close to those considered by Ricard & Froidevaux (1986). The growth-rate factor reaches 150 and the deformation pattern corresponds to buckling or boudinage of the upper competent layer.

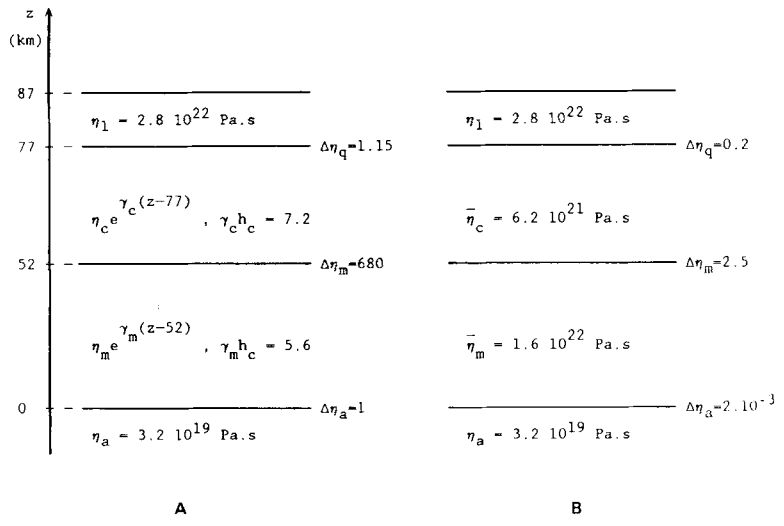

Figure 10. Comparison of exponential-viscosity and constant-viscosity models. Model A is the same as in Fig. 4(a) ($q_m = 40\,\mathrm{mW\,m^{-2}}$, $H_s = 4\,\mu\mathrm{W\,m^{-3}}$, $\dot{\varepsilon}_{xx} = 10^{-15}\,\mathrm{s^{-1}}$) with an exponentially decreasing viscosity in the ductile layers. In model B, viscosities are constant and are obtained by replacing the exponential viscosities by their average value in the layer.

instability of the upper crust, while the deepest layers passively follow the deformation. A similar pinch and swell deformation is observed for the second peak, with practically no deformation of the underlying layers. Finally, the last maximum corresponds to the formation of 'folds' in the upper crust without deformation at depth.

The style of deformation is clearly very different from the one we observe. The comparison of the parameter values, however, is not straightforward since the mechanical model is not the same: here the fluids are considered as non-Newtonian ($n \neq 1$), but viscosity in the basic state of uniform stretching is supposed to be constant.

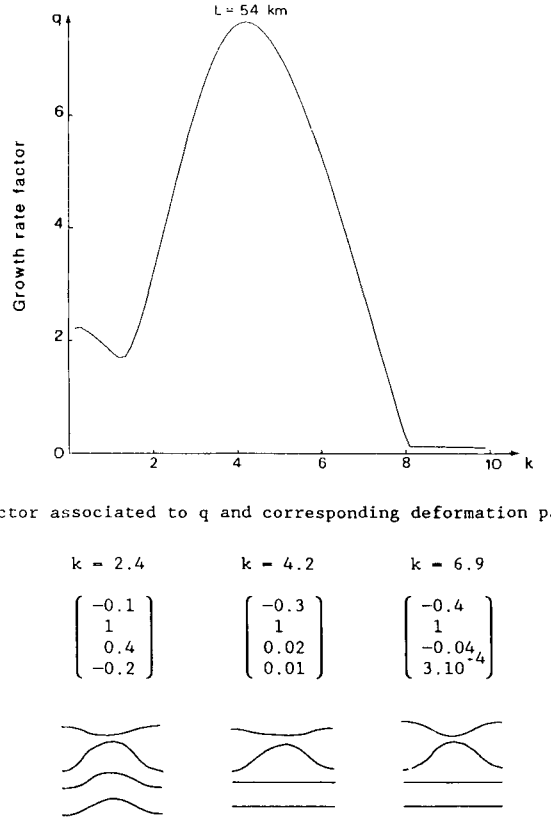

Figure 11. Growth-rate factor and modes of deformation for the model of lithosphere illustrated in Fig. 10(B). The present results should be compared with Fig. 4(a). The change of viscosity law not only affects the value of q, but modifies the associated deformation pattern which depends now on the wave number. For intermediate values of k (and, in particular, for $k = 4.2$ for which q is maximized) an unstable behaviour of the upper crust is observed.

Our first question concerns the influence of the viscosity law. The two models presented in Fig. 10 are different approximations of the same physical structure, that is a lithosphere with a $80\,mW\,m^{-2}$ surface heat-flow and a strength stratification derived from the model of Brace & Kohlstedt (1980). The first approximation is the one we have used until now, with exponential viscosity laws in the ductile layers; in the second, these laws have been replaced by constants, equal to the average of the exponential viscosities within the layer where they apply. The evolution of growth rate factor q for this second situation (Fig. 11) differs significantly from the first one (Fig. 4). The amplification is less efficient, since q is smaller, but a mechanical instability of boudinage-type is observed for the upper crust at intermediate wave numbers, whereas it was only gravitational, at any wavelength, for exponential viscosity laws.

It seems therefore that the rheological approximations used in the models to describe a given structure may greatly influence the results. Zuber *et al.* (1986), making a similar test, do not reach the same conclusion. These workers compare two models in which the strength of the substratum beneath a single strong layer (1) either decreases exponentially with depth (C model), or (2) decreases discontinuously to a lower uniform value at the bottom of the layer (J model). They conclude that these two approximations predict similar physical behaviour for wave numbers of interest, and similar dominant wavelengths. However, unlike the test illustrated in Figs 10 and 11, Zuber *et al.* (1986) do not look for a real correspondence between the continuous and jump models being compared. The parameters describing both of them are chosen independently and are favourable to the growth of an instability. As it is well established, by these authors in particular, that the dominant wavelengths are primarily determined by the layer thicknesses, the small influence of the model observed by Zuber *et al.* (1986) is not really surprising.

An exponential viscosity law seems more appropriate to approximate the strength in the ductile part of the lithosphere and the results obtained with it should be more reliable than those which correspond to constant viscosities. But it cannot be ruled out that other assumptions have a determining importance, like for example the choice of the equivalent viscosity in the brittle layers.

Beyond this problem of modelling the lithosphere, it is interesting to notice that, in our case, the brittle layers are not stronger than the immediately underlying medium, contrary to what is assumed by other authors. As a consequence, the values of S_s and S_M are high and the ratios $\Delta\eta_q$ and $\Delta\eta_0$ are greater than 1. Let us imagine that the strength of the brittle layers is 10 times greater than the value we assumed. Given the uncertainties about the exact lithospheric rheology such an error is quite possible. This test has been performed for a three-layer lithosphere (Fig. 12) and a four-layer one (Fig. 13). The maximum value of q significantly increases and corresponds to an instability of the upper crust. This result is consistent with the conditions of instability proposed by Fletcher & Hallet (1983), since

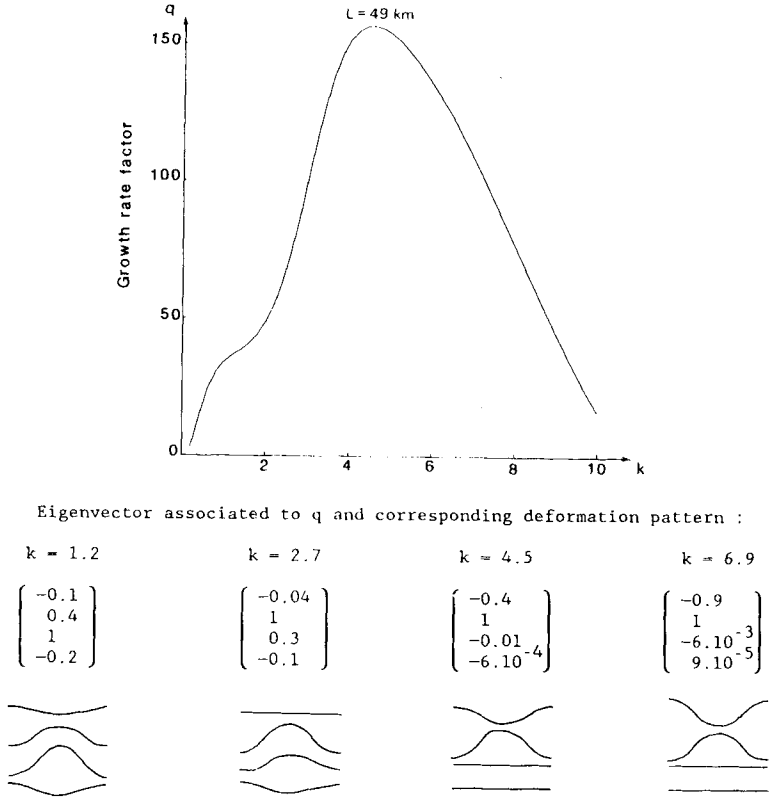

Figure 12. Same plot as in Fig. 11 but for a model of lithosphere where the strength of the upper crust has been multiplied by a factor of 10 with respect to the value of Fig. 4(a) so that $\Delta\eta_q = 0.1$, $S_s = 0.8$, $S_M = 0.1$ and $S_L = -0.01$, the other features being unchanged. For these values, the lithosphere is unstable with respect to tension, and boudinage-like instabilities of the upper crust can develop at any considered wave number, with a maximum rate of growth for $k = 4.5$.

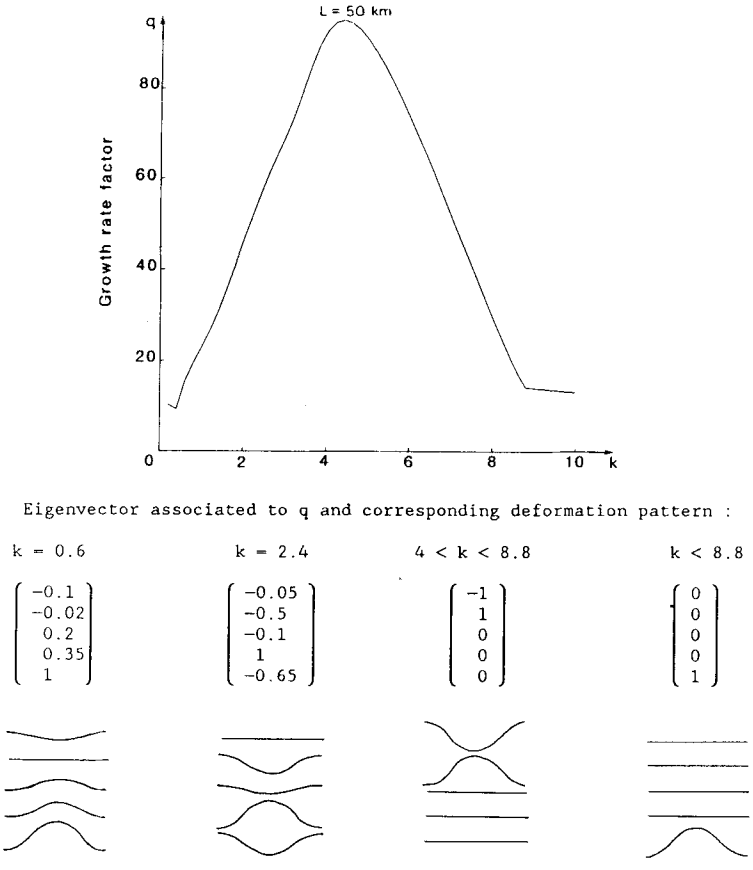

Figure 13. Same test as in Fig. 12 but for a four-layer model of lithosphere. The parameter values correspond to $q_m = 30\,\mathrm{mW\,m^{-2}}$, $H_s = 4\,\mu\mathrm{W\,m^{-3}}$, $\dot{\varepsilon}_{xx} = 10^{-15}\,\mathrm{s^{-1}}$ (see Fig. 5a), but the strength of the brittle layers is 10 times greater, so that $\Delta\eta_q = 0.2$, $\Delta\eta_M = 2190$, $\Delta\eta_0 = 0.2$, $S_s = 0.8$, $S_M = 0.1$ and $S_L = -0.01$. As in Fig. 12, stretching instabilities can grow with these new parameter values.

this new choice of strength changes the value of S_s and $\Delta\eta_q$ so that:

$$S_s < \gamma_c h_c$$

and

$$\Delta\eta_q < 1.$$

The preceding discussion is by no means exhaustive since we did not investigate systematically the influence of the various parameters. This has been done by Zuber *et al.* (1986) and Ricard & Froidevaux (1986) for a wide range of parameter values, all favourable to an unstable extension of the lithosphere. But these values are not unique; our study demonstrates that other estimates, best constrained by experimental results on rock mechanics, lead to slightly different conclusions. The above test however shows that the strengths of the various layers are determining factors, as yet insufficiently constrained by the data.

NON-SINUSOIDAL PERTURBATION OF THE INTERFACES

The spectral analysis presented above illustrates that the eventual amplification of an initial small-scale topography is selective, the dominant wavelengths being more or less simply determined by the layer thicknesses. Furthermore, the preferential mode of deformation (which is associated with the growth rate factor q) depends on the wavelength. If the preceding model could apply to continuing evolution (it is actually limited to the initial stages of the deformation), the affected interfaces would show, after a certain time, a sinusoidal undulation with a wavelength L_d corresponding to the maximum of the curve $q(L)$. In addition, the respective amplitudes of the interfaces would be proportional to the eigenvector associated with $q(L_d)$. However, the method does not allow us to compute final deformation and therefore to predict *a priori* the long term evolution of an initial, non-sinusoidal, relief of the interfaces. As far as the early evolution is concerned, the resulting geometry will depend on, among other things, the initial spectral content, the differences between the eigenvalues, and the interface (or interfaces) which is initially deformed.

For our model of lithospheric structure and behaviour, however, we showed that the only positive eigenvalue is associated with an instability of the lithosphere–asthenosphere boundary, at any wavelength. Then, it is probable that, whatever the exact shape of this interface, it will be amplified when the lithosphere is stretched. As an example, let us examine the early evolution of an initially Gaussian topography of the form:

$$h(x) = h_0 \exp(-x^2/2D^2).$$

We have chosen this function because of its simple spectrum, but also in order to approximate a local

constriction. Since the problem has been linearized for the first stages of the deformation, the evolution of vector **H** through time can be computed without particular difficulty if all the interfaces exhibit a Gaussian relief, characterized by the same parameter D (see Appendix C). Note that the spectrum of this topography includes the zero frequency: for this limit value, it has been shown (Bassi 1986) that all the eigenvalues vanish. This means that the average of the topography is independent of time and probably results from the incompressibility hypothesis.

Let us suppose then that the lithosphere–asthenosphere boundary shows a small-scale upwelling represented by a Gaussian function of parameter $D = 35$ km. For this value of D, the amplitude of the interface is reduced by a factor 100 for a distance $x = 106$ km, that is to say a global extent of the perturbation of approximately 200 km. Fig. 14 shows the position of the various interfaces through time for a model of lithosphere with a surface heat-flow of 80 mW m^{-2} and a mean rate of deformation equal to 10^{-16} s^{-1}. After a global deformation $\dot{\varepsilon}_{xx}t$ of 15 per cent (which is supposed to produce little modification of lithospheric structure), the central upwelling is amplified by a factor of seven whereas the other interfaces remain approximately flat, as expected. The base of the lithosphere presents alternate highs and lows, the amplitude of which rapidly decreases away from the central uplift.

This behaviour, however, is not very encouraging as far as sedimentary-basin formation is concerned, since it does not introduce any modification of the crust thickness and consequently does not lead to subsidence. A model of the lithosphere described by the parameter values of Fig. 12, obtained by increasing the strength of the upper crust, is more interesting from this point of view as the lithosphere exhibits modes of deformation in which the crust presents local constrictions. Let us examine the behaviour of such a structure, for example when the upper brittle crust shows a weak initial neck of approximately 100 km extent ($D =$ 17.5 km). The results are presented on Fig. 15. The structure appears to be highly unstable with respect to tension since, for a global deformation of only 3 per cent, the position of the brittle–ductile transition in the crust is amplified by a factor of 20. This interface shows an oscillation which progressively decays; its wavelength, close to 50 km, corresponds to the maximum of the curve $q(k)$ (Fig. 12). The upper crust is characterized by a series of constrictions, the principal (for $x = 0$) being greatly amplified with respect to its initial form. In addition, it is narrower than it was initially. The crust as a whole is thinned at the centre of the initial neck: the Moho has the form of an upward bulge, centred on $x = 0$, and with a lateral extent equal to the initial width of the neck.

These two examples illustrate the consequences of the above spectral analysis results on the early evolution of a more 'realistic' (actually, still theoretical...) initial topography. Of course, these results are essentially qualitative and will probably depend on the exact frequency spectrum of the topography, e.g. on the parameter D. Nevertheless, they could have some interesting developments if the upper crust is regarded as a competent layer with respect to the lower crust. In any case, it is important to keep in mind the limits of the method which is supposed to give initial tendencies rather than final deformations.

CONCLUSION

Our study, when compared with the previous, similar studies by Zuber *et al.* (1986) and Ricard & Froidevaux (1986), clearly shows the extent to which certain rheological hypotheses are central for the results of geodynamical models. It will be difficult to draw any definite conclusions concerning the lithosphere's ability to deform until its rheology is better known. The model used by us is a compromise between the complexity of continental lithosphere rheology, as described by Brace & Kohlstedt (1980)

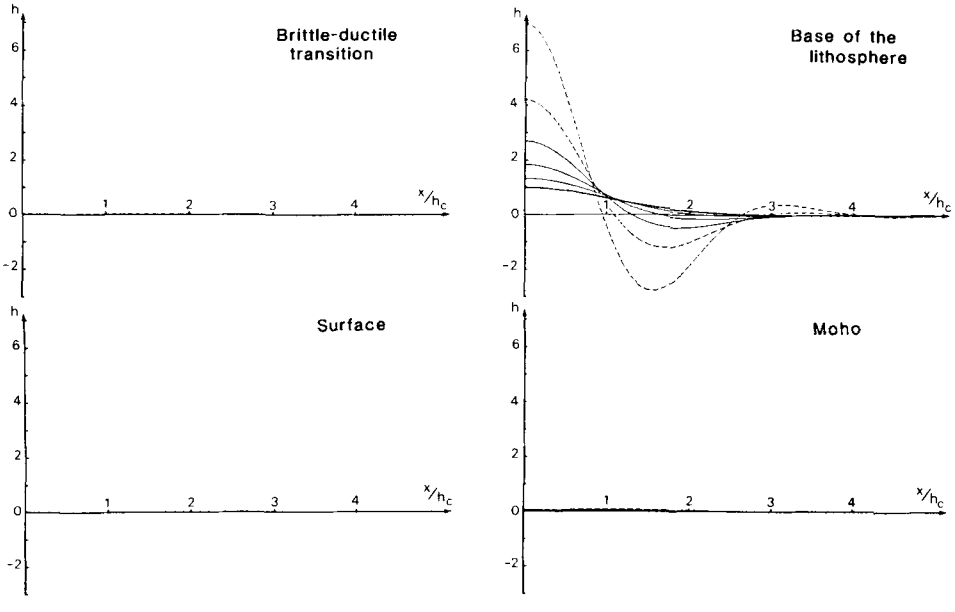

Figure 14. Position of the interfaces of a stretched lithosphere through time when, initially, the lithosphere–asthenosphere boundary shows a Gaussian upwelling of parameter $D = h_c = 35$ km, the other interfaces being flat. The model of lithosphere corresponds to $q_m = 40$ mW m^{-2}, $H_s = 4\,\mu$W m^{-3}, $\dot{\varepsilon}_{xx} = 10^{-16}$ s^{-1}. The time interval between the curves corresponds to a mean deformation $\dot{\varepsilon}_{xx}\Delta t \simeq 0.03$.

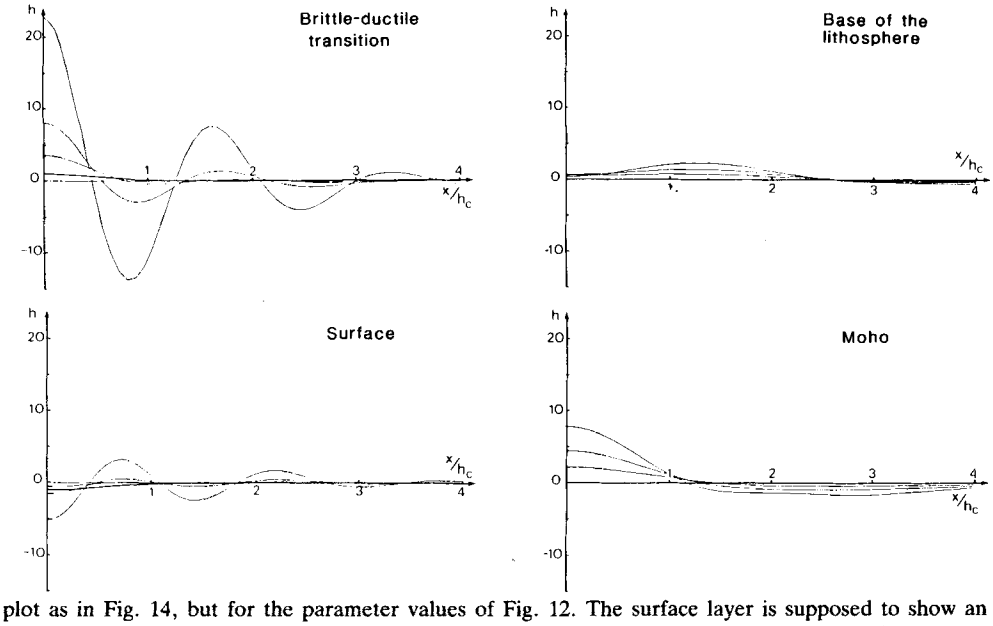

Figure 15. Same plot as in Fig. 14, but for the parameter values of Fig. 12. The surface layer is supposed to show an initial neck which is schematically represented by a Gaussian perturbation of the surface and the brittle–ductile transition. The time interval between the curves corresponds to a mean deformation $\dot{\bar{\varepsilon}}_{xx}\Delta t = 0.01$.

among others and the approximations required for an analytic study of non-uniform extension. On the basis of our model, we cannot conclude that the lithosphere is unstable with respect to necking; the only instability for which we have evidence results from the gravitational instability of the asthenosphere with respect to the cooler mantle lithosphere. The model, however, is highly sensitive to the parameter values and, particularly, to the strength stratification. If an order-of-magnitude error is made in the evaluation of the brittle layer strengths, the conclusions are quite different and extension becomes unstable.

In connection with this, it is important to emphasize the fundamental role played by the brittle layers in this discussion of mechanical instability, essentially because they are approximated by power-law fluids with very large stress exponents. This result is questionable since the preceding mechanical description relies on a number of assumptions. In addition, it contradicts the common idea that the mechanical importance of the brittle upper crust is only minor and that the crust passively follows the extension of the ductile lithosphere. It would be interesting, therefore, to test further the influence of this mechanical approximation on the results, and to evaluate the exact role of the crust in the deformation.

Laboratory experiments have demonstrated that the conditions of growth of a necking instability depend on the details of geometry and structure of the sample. A similar characteristic may be observed in our theoretical analysis, since it appears that slight changes in the assumptions not only affect the precision of the results but modify them fundamentally. It is therefore necessary to define a formalism which will take into account the progressive evolution of the parameters with depth, and avoid, as far as possible, the artificial discontinuities of strength or density.

Finally, the perturbation method does not allow the working out of the long-term evolution of an initial configuration. As the deformation proceeds there is certainly a wavelength selection, as our spectral analysis suggests. However, the thermal, and therefore rheological, modifications introduced by an important stretching will change the dominant wavelengths through time, so that the final effect is not obvious. The problem of long-term deformation is mathematically much more complicated than the analysis we have presented, as it is non-linear and coupled with a thermal problem; it has to be addressed with numerical methods, such as finite-element methods. However, this complexity is probably difficult to avoid in attempting a closer understanding of lithospheric deformation.

ACKNOWLEDGMENTS

This research was supported by IFREMER (formerly CNEXO) under grants 84-7603 and 85-2-410398/DERO/GM. We thank an anonymous reviewer for helpful comments on the manuscript.

REFERENCES

Artemjev, M. E. & Artyushkov, E. V., 1971. Structure and isostasy of the Baikal rift and the mechanism of rifting, *J. geophys. Res.*, **76,** 1197–1211.

Bassi, G., 1986. Contribution à l'étude de la déformation de la lithosphère associée à la formation des bassins sédimentaires et des marges continentales passives, *Doctoral Thesis,* University of Strasbourg, France.

Beaumont, C., Keen, C. E. & Boutilier, R., 1982. On the evolution of rifted continental margins: comparison of models and observations for the Nova Scotian margin, *Geophys. J.R. astr. Soc.*, **70,** 667–715.

Brace, W. F. & Kohlstedt, D. L., 1980. Limits on lithospheric stress imposed by laboratory experiments, *J. geophys. Res.*, **85,** 6248–6252.

Campbell, J. D., 1967. Plastic instability in rate dependent materials, *J. Mech. Phys. Solids,* **15,** p. 359.

Cochran, J. R., 1983. Effects of finite rifting times on the development of sedimentary basins, *Earth planet. Sci. Lett.*, **66,** 289–302.

Fletcher, R. C. & Hallet, B., 1983. Unstable extension of the

lithosphere: a mechanical model for Basin-and-Range structure, J. geophys. Res., **88,** 7457–7466.
Foucher, J. P., Le Pichon, X. & Sibuet, J. C., 1982. The ocean continent transition in the uniform lithospheric stretching model: role of partial melting in the mantle, *Phil. Trans. R. Soc. A*, **305,** 27–43.
Goetze, C. & Evans, B., 1979. Stress and temperature in the bending lithosphere as constrained by experimental rock mechanics, *Geophys. J.R. astr. Soc.*, **59,** 463–478.
Hart, E. W., 1967. Theory of the tensile test, *Acta Met.*, **15,** p. 351.
Jaeger, J. C. & Cook, N. G. W., 1976. *Fundamentals of Rock Mechanics,* John Wiley, New York.
Jalinier, J. M., 1981. Mise en forme et endommagement, *Doctoral Thesis,* University of Metz, France.
Keen, C. E., 1981. The continental margins of eastern Canada: a review, in *Dynamics of Passive Margins,* ed. Scrutton, R. A., *Geodynamics Series,* **6,** 45–58, American Geophysical Union, Washington, DC.
Keen, C. E. & Barrett, D. L., 1981. Thinned and subsided continental crust on the rifted margin of eastern Canada: crustal structure, thermal evolution and subsidence history, *Geophys. J.R. astr. Soc.*, **65,** 443–465.
Kirby, S. H., 1983. Rheology of the lithosphere, *Rev. Geophys. Space Phys.*, **21,** 1458–1487.
Kusznir, N. J. & Park, R. G., 1982. Intraplate lithosphere strength and heat flow, *Nature,* **299,** 540–542.
Kusznir, N. J. & Park, R. G., 1984. The strength of intraplate lithosphere, *Phys. Earth planet. Int.*, **36,** 224–235.
McKenzie, D., 1978. Some remarks on the development of sedimentary basins, *Earth planet. Sci. Lett.*, **40,** 25–32.
Morgan, P. & Sass, J. H., 1984. Thermal regime of the continental lithosphere, *J. Geodynamics,* **1,** 143–166.
Ricard, Y. & Froidevaux, C., 1986. Stretching instabilities and lithospheric boudinage, *J. geophys. Res.*, **91,** 8314–8324.
Rossard, C., 1966. Formation de la striction dans la déformation à chaud par traction, *Rev. Met.*, **63,** 225.
Royden, L. & Keen, C. E., 1980. Rifting process and thermal evolution of the continental margin of eastern Canada determined from subsidence curves, *Earth planet. Sci. Lett.*, **51,** 343–361.
Sawyer, D. S., 1985. Brittle failure in the upper mantle during extension of continental lithosphere, *J. geophys. Res.*, **90,** 3021–3025.
Smith, R. B., 1977. Formation of folds, boudinage, and mullions in non-newtonian materials, *Bull. geol. soc. Am.*, **88,** 312–320.
Turcotte, D. L. & Schubert, G., 1982. *Geodynamics; Applications of Continuum Physics to Geological Problems,* John Wiley, New York.
Vink, G. E., Morgan, W. J. & Zhao, W. L., 1984. Preferential rifting of continents: a source of displaced terranes, *J. geophys. Res.*, **89,** 10072–10076.
Zuber, M. T., Paramentier, E. M. & Fletcher, R. C., 1986. Extension of continental lithosphere: a model for two scales of Basin and Range deformation, *J. geophys. Res.*, **91,** 4826–4838.

APPENDIX A

Solution of the perturbing flow problem

We want to solve the Navier–Stokes equations for the plane perturbing flow (equation 15), in a medium described by the constitutive equations (14). The viscosity in the basic state of uniform extension, $\bar{\eta}$, is either exponential or constant. Except in the asthenosphere, the stress exponent $n \neq 1$.

Let $\tilde{u}$ and $\tilde{w}$ be the horizontal and vertical components of the velocity. The incompressibility condition (16) is satisfied by the separable solution:

$$\tilde{w}(x, z) = W(z) \cos \lambda x, \qquad \tilde{u}(x, z) = -W'(z)(\sin \lambda x/\lambda). \tag{A1}$$

1 Exponential viscosity law

When $\bar{\eta}$ is an exponential function of depth (equation 10), $W(z)$ must be a solution of the fourth-order differential equation (Fletcher & Hallet 1983):

$$\frac{d^4W}{dz^4} + 2\gamma \frac{d^3W}{dz^3} + \left[\gamma^2 - 2\lambda^2\left(\frac{2}{n} - 1\right)\right] \frac{d^2W}{dz^2} - 2\gamma\lambda^2\left(\frac{2}{n} - 1\right) \frac{dW}{dz} + \lambda^2(\gamma^2 + \lambda^2)W = 0, \tag{A2}$$

where γ is the inverse of the viscosity decay length. A general solution of this equation is:

$$W(z) = A_1 \cos \beta\lambda z \exp(\alpha'\lambda z) + A_2 \frac{\sin \beta\lambda z}{\beta\lambda} \exp(\alpha'\lambda z) + A_3 \cos \beta\lambda z \exp(\alpha''\lambda z) + A_4 \frac{\sin \beta\lambda z}{\beta\lambda} \exp(\alpha''\lambda z) \tag{A3}$$

with

$$m = \frac{\gamma}{\lambda}$$

$$a = \frac{2^{1/2}}{2}\left(\frac{m^2}{4} + \frac{2}{n} - 1 + \left[\frac{m^4}{16} + \frac{m^2}{2}\left(\frac{2}{n} + 1\right) + 1\right]^{1/2}\right)^{1/2}$$

$$r = \left(\frac{m^2}{4} + \frac{n-1}{n^2}\right)^{1/2}$$

$$\beta = r/a$$

$$\alpha' = a - m/2$$

$$\alpha'' = -a - m/2.$$

In the preceding expression, $W(z)$ is developed on a basis of the solutions of (A2), which is slightly different from the one proposed by Fletcher & Hallet (1983). We had better choose a family of independent solutions which is continuous for $\lambda \to 0$, since the limit value $\lambda = 0$ may intrude in the case of a non-sinusoidal perturbation of the interfaces (see Appendix C).

The general expressions for $\tilde{u}$, $\tilde{w}$, $\tilde{\sigma}_{xz}$ and $\tilde{\sigma}_{zz}$ are derived from $W(z)$ and the constitutive equations (14), and are as follows:

$$\tilde{w}(x, z) = \left[A_1 \cos \beta\lambda z \exp(\alpha'\lambda z) + A_2 \frac{\sin \beta\lambda z}{\beta\lambda} \exp(\alpha'\lambda z) + A_3 \cos \beta\lambda z \exp(\alpha''\lambda z) + A_4 \frac{\sin \beta\lambda z}{\beta\lambda} \exp(\alpha''\lambda z)\right] \cos \lambda x \tag{A4}$$

$$\tilde{u}(x, z) = \left\{-\left(\left[\alpha' A_1 + \frac{A_2}{\lambda}\right] \cos \beta\lambda z + \left[\frac{\alpha' A_2}{\beta\lambda} - \beta A_1\right] \sin \beta\lambda z\right) \exp(\alpha'\lambda z) - \left(\left[\alpha'' A_3 + \frac{A_4}{\lambda}\right] \cos \beta\lambda z + \left[\frac{\alpha'' A_4}{\beta\lambda} - \beta A_3\right] \sin \beta\lambda z\right) \exp(\alpha''\lambda z)\right\} \sin \lambda x \tag{A5}$$

$$\bar{\sigma}_{xz}(x, z) = -\bar{\eta}\lambda \sin \lambda x$$
$$\times \left\{ \left(\left[(1 + \alpha'^2 - \beta^2)A_1 + \frac{2\alpha'}{\lambda} A_2 \right] \cos \beta\lambda z \right.\right.$$
$$\left. + \left[-2\alpha'\beta A_1 + \frac{(1 + \alpha'^2 - \beta^2)}{\beta\lambda} A_2 \right] \sin \beta\lambda z \right) \exp(\alpha'\lambda z)$$
$$+ \left(\left[(1 + \alpha''^2 - \beta^2)A_3 + \frac{2\alpha''}{\lambda} A_4 \right] \cos \beta\lambda z \right.$$
$$\left.\left. + \left[-2\alpha''\beta A_3 + \frac{(1 + \alpha''^2 - \beta^2)}{\beta\lambda} A_4 \right] \sin \beta\lambda z \right) \exp(\alpha''\lambda z) \right\} \tag{A6}$$

$$\bar{\sigma}_{zz}(x, z) = \bar{\eta}\lambda \left\{ \left(\left[M_1 A_1 + \frac{M_2}{\beta\lambda} A_2 \right] \cos \beta\lambda z \right.\right.$$
$$\left. + \left[\frac{M_1}{\beta\lambda} A_2 - M_2 A_1 \right] \sin \beta\lambda z \right) \exp(\alpha'\lambda z)$$
$$+ \left(\left[M_3 A_3 + \frac{M_4}{\beta\lambda} A_4 \right] \cos \beta\lambda z \right.$$
$$\left.\left. + \left[\frac{M_3}{\beta\lambda} A_4 - M_4 A_3 \right] \sin \beta\lambda z \right) \exp(\alpha''\lambda z) \right\} \cos \lambda x, \tag{A7}$$

where:

$$M_1 = \left(\frac{4}{n} - 1 \right) \alpha' - m(1 + \alpha'^2 - \beta^2) - \alpha'(\alpha'^2 - 3\beta^2)$$

$$M_2 = \beta \left[\left(\frac{4}{n} - 1 \right) - 2\alpha' m + (\beta^2 - 3\alpha'^2) \right]$$

and M_3 and M_4 are evaluated by replacing α' by α'' in M_1 and M_2, respectively.

2 *Constant viscosity* η_0

The differential equation (A2) regularly depends on the parameter γ, so that a general solution for the constant viscosity case may be directly obtained by setting $\gamma = 0$ in the above relations. It is more convenient however, for numerical reasons, to develop $W(z)$ on the basis of solutions which are continuous in the limit process $\lambda \to 0$, e.g.

$$W(z) = B_1 \cos \beta_1\lambda z \cosh \alpha_1\lambda z + B_2 \frac{\sin \beta_1\lambda z}{\beta_1\lambda} \cosh \alpha_1\lambda z$$
$$+ B_3 \frac{\sin \beta_1\lambda z}{\alpha_1\beta_1\lambda^2} \sinh \alpha_1\lambda z - B_4 \frac{3}{\alpha_1\lambda^3}$$
$$\times \left[\cos \beta_1\lambda z \sinh \alpha_1\lambda z - \frac{\alpha_1}{\beta_1} \sin \beta_1\lambda z \cosh \alpha_1\lambda z \right], \tag{A8}$$

where

$$\alpha_1 = n^{-1/2} \quad \text{and} \quad \beta_1 = (1 - 1/n)^{1/2}.$$

The velocity and stress components may then be written in the form:

$$\bar{w}(z) = \left(B_1 \cos \beta_1\lambda z \cosh \alpha_1\lambda z + B_2 \frac{\sin \beta_1\lambda z}{\beta_1\lambda} \cosh \alpha_1\lambda z \right.$$
$$+ B_3 \frac{\sin \beta_1\lambda z}{\alpha_1\beta_1\lambda^2} \sinh \alpha_1\lambda z - B_4 \frac{3}{\alpha_1\lambda^3}$$
$$\left. \times \left[\cos \beta_1\lambda z \sinh \alpha_1\lambda z - \frac{\alpha_1}{\beta_1} \sin \beta_1\lambda z \cosh \alpha_1\lambda z \right] \right) \cos \lambda x \tag{A9}$$

$$\bar{u}(x, z) = -\sin \lambda x \left(\frac{B_2}{\lambda} \cos \beta_1\lambda z \cosh \alpha_1\lambda z \right.$$
$$+ \left[\alpha_1 B_1 + \frac{B_3}{\alpha_1\lambda^2} \right] \cos \beta_1\lambda z \sinh \alpha_1\lambda z$$
$$+ \left[-\beta_1 B_1 + \frac{B_3}{\beta_1\lambda^2} \right] \sin \beta_1\lambda z \cosh \alpha_1\lambda z$$
$$\left. + \left[\frac{\alpha_1}{\beta_1} \frac{B_2}{\lambda} + \frac{3}{\alpha_1\beta_1\lambda^3} B_4 \right] \sin \beta_1\lambda z \sinh \alpha_1\lambda z \right) \tag{A10}$$

$$\bar{\sigma}_{xz}(x, z) = -\eta_0 \left(\left[\frac{2}{n_1} \lambda B_1 + \frac{2B_3}{\lambda} \right] \cos \beta_1\lambda z \cosh \alpha_1\lambda z \right.$$
$$+ 2\alpha_1 B_2 \cos \beta_1\lambda z \sinh \alpha_1\lambda z$$
$$+ \left[-2\alpha_1\beta_1\lambda B_1 + \frac{2}{n_1} \frac{B_3}{\alpha_1\beta_1\lambda} \right] \sin \beta_1\lambda z \sinh \alpha_1\lambda z$$
$$\left. + \left[\frac{2}{n_1} \frac{B_2}{\beta_1} + \frac{6B_4}{\beta_1\lambda^2} \right] \sin \beta_1\lambda z \cosh \alpha_1\lambda z \right) \sin \lambda x \tag{A11}$$

and finally

$$\bar{\sigma}_{zz}(x, z) = \eta_0 \cos \lambda x \left(-\frac{6B_4}{\lambda^2} \cos \beta_1\lambda z \cosh \alpha_1\lambda z \right.$$
$$+ \frac{2B_3}{\beta_1\lambda} \sin \beta_1\lambda z \cosh \alpha_1\lambda z$$
$$+ 2\lambda\alpha_1 B_1 \cos \beta_1\lambda z \sinh \alpha_1\lambda z$$
$$\left. + \left[\frac{2\alpha_1}{\beta_1} B_2 + \frac{6B_4}{\alpha_1\beta_1 n_1\lambda^2} \right] \sin \beta_1\lambda z \sinh \alpha_1\lambda z \right) \tag{A12}$$

3 *Newtonian fluid*

This case corresponds to the particular value $n = 1$ with respect to the preceding examples. Since (A2) regularly depends on n, the solutions are obtained by setting $n = 1$, and hence $\beta_1 = 0$, in relations (A9) to (A12). Consequently,

$$\bar{w}(x, z) = \cos \lambda x \left[C_1 \cosh \lambda z + C_2 \cosh \lambda z + \right.$$
$$\left. + C_3 z \frac{\sinh \lambda z}{\lambda} - \frac{3}{\lambda^3} C_4 (\sinh \lambda z - \lambda z \cosh \lambda z) \right] \tag{A13}$$

$$\tilde{u}(x, z) = -\sin \lambda x\left(\left[C_1 + \frac{C_3}{\lambda^2}\right]\sinh \lambda z + \frac{C_2}{\lambda}\cosh \lambda z + \frac{C_3}{\lambda} z \cosh \lambda z + \left[C_2 + \frac{3C_4}{\lambda^2}\right] z \sinh \lambda z\right) \quad \text{(A14)}$$

$$\tilde{\sigma}_{xz}(x, z) = -\eta_0 \sin \lambda x\left(\left[2\lambda C_1 + \frac{2C_3}{\lambda}\right]\cosh \lambda z + 2C_3 z \sinh \lambda z + 2C_2 \sinh \lambda z + \left[2\lambda C_2 + \frac{6C_4}{\lambda}\right] z \cosh \lambda z\right) \quad \text{(A15)}$$

$$\tilde{\sigma}_{zz}(x, z) = \eta_0 \cos \lambda x\left(2C_3 z \cosh \lambda z + 2\lambda C_1 \sinh \lambda z - \frac{6C_4}{\lambda^2}\cosh \lambda z + \left[2\lambda C_2 + \frac{6C_4}{\lambda}\right] z \sinh \lambda z\right). \quad \text{(A16)}$$

If m is the number of layers of the problem, the final solution for the perturbing flow requires the determination of $4m$ integration constants. Boundary conditions (17) to (20) provide $4(m-1)$ relations. At the free surface, the normal and shear stresses vanish, thus providing two supplementary conditions. Finally, the assumption of no slip at the base of the asthenosphere ($\tilde{u} = 0$, $\tilde{w} = 0$) completes the set of required equations. All these conditions are linear with respect to the integration coefficients, so that the problem reduces to the solution of a $4m$-order linear system.

APPENDIX B

Lithospheric strength versus depth for a given rate of deformation

We explain here the construction of the typical strength profile illustrated on Fig. 1. This variation of stress with depth is a consequence of a few principles suggested by Goetze & Evans (1979), or Brace & Kohlstedt (1980) for the continental case, referred to in the text. The deviatoric stress ($\bar{\sigma}_{xx} - \bar{\sigma}_{zz}$) is directly computed into the ductile parts of the lithosphere when a characteristic flow-law for the crust and the mantle, a model of geotherm, and a rate of deformation have been defined. The brittle case is somewhat more complicated: the recasting of Byerlee's law in a strength versus depth relation relies on some implicit assumptions that we wish to emphasize.

Let us assume, for example, that there is no fluid pore-pressure. In terms of principal stresses, Byerlee's law is:

$$\begin{cases} T_1 = 5T_3 & \text{if} \quad T_3 < 110\,\text{MPa} \\ T_1 = 3.1T_3 + 210 & \text{if} \quad T_3 > 110\,\text{MPa} \end{cases} \quad \text{(B1)}$$

where T_1 and T_3 are the principal maximum and minimum stresses, respectively. It is important to stress that the preceding law uses the rock mechanics sign convention which considers compression as positive. T_{ij} is the total stress tensor, let us say:

$$T_{ij} = \sigma_{ij} + p_0 \delta_{ij}, \quad \text{(B2)}$$

where p_0 is the hydrostatic stress due to the gravity field, and σ_{ij} is the tectonic stress.

If plane strain is assumed, with no deformation along the y axis, T_{yy} is the intermediate principal stress. In addition, when the structure is submitted to tension along the x axis:

$$T_1 = T_{zz} \quad \text{(B3)}$$

if T_{zz} is supposed to be a principal stress (this is rigourously true if the deformation is of pure shear type). Then:

$$T_3 = T_{xx}. \quad \text{(B4)}$$

As T_3 is negative when the structure is stretched, it is always less than 110 MPa, and consequently:

$$\sigma_{zz} - \sigma_{xx} = T_1 - \frac{T_1}{5} = \tfrac{4}{5}T_1 = \tfrac{4}{5}T_{zz}. \quad \text{(B5)}$$

Assuming that the vertical stress T_{zz} does not differ much from the gravitational stress p_0, relation (B5) may be written in the form:

$$\sigma_{zz} - \sigma_{xx} = \tfrac{4}{5}p_0 = \tfrac{4}{5}\rho g d, \quad \text{(B6)}$$

where d is the depth of burial (counted positively downwards, from the surface). With the usual sign convention of solid mechanics, the deviatoric stress is finally:

$$\bar{\sigma}_{xx} - \bar{\sigma}_{zz} = \tfrac{4}{5}\rho g d \quad \text{(B7)}$$

With a density of 2.8 g cm^{-3} for the crust and 3.3 g cm^{-3} for the mantle, this law becomes:

$$\bar{\sigma}_{xx} - \bar{\sigma}_{zz} = 22.4d. \quad \text{(B8)}$$

in the crust, with d in km and $\bar{\sigma}_{xx} - \bar{\sigma}_{zz}$ in MPa, and in the mantle:

$$\bar{\sigma}_{xx} - \bar{\sigma}_{zz} = 22.4d_c + 26.4(d - d_c)$$

if d_c is the depth of Moho discontinuity.

One can thus define a strength versus depth relation for each typical mode of deformation in the lithosphere. The stress profile and associated rheological stratification of Fig. 1 results from these relations and from the assumption that the mechanism that requires the least stress is dominant at each depth.

APPENDIX C

Evolution of the amplitude vector H through time for a Gaussian perturbation of the interfaces

Let $h_i(x)$, the topography of the ith interface, be a Gaussian function of parameter D, i.e.

$$h_i(x) = h_{i0} \exp -(x^2/2D^2). \quad \text{(C1)}$$

Taking into account the reciprocity of the Fourier transformation, $h_i(x)$ may be developed as a function of its Fourier transform, and satisfies:

$$h_i(x) = h_{i0}\left(\frac{2}{\pi}\right)^{1/2} D \int_0^\infty \exp\left(-\frac{D^2\lambda^2}{2}\right)\cos \lambda x \, d\lambda. \quad \text{(C2)}$$

Let us now assume that all the interfaces of the problem present a Gaussian disturbance with respect to a planar geometry, and that these functions only differ by their amplitude h_{i0}. Then, the amplitude vector **H** may then be

written in the form:

$$\mathbf{H}(x, t=0) = \left(\frac{2}{\pi}\right)^{1/2} D \int_0^\infty \exp\left(-\frac{D^2\lambda^2}{2}\right)\mathbf{H}_0(t=0)\cos\lambda x\, d\lambda. \tag{C3}$$

The evolution of $\mathbf{H}_0$ through time has been determined in the text for each wave number λ; according to equation (23):

$$\mathbf{H}_0(t) = \sum_{j=1}^{m} a_{0j}(\lambda)\exp\left(q_j(\lambda)\hat{\varepsilon}_{xx}t\right)\mathbf{V}_j(\lambda) \tag{C4}$$

where $q_j(\lambda)\hat{\varepsilon}_{xx}$ and $\mathbf{V}_j(\lambda)$ are the eigenvalues and eigenvectors corresponding to λ, and the constants a_{0j} are the coefficients of the decomposition of $\mathbf{H}_0$ on the eigenvector basis.

Since the problem has been linearized, the vector $\mathbf{H}$ at time t satisfies:

$$\mathbf{H}(x, t) = \left(\frac{2}{\pi}\right)^{1/2} D \int_0^\infty \left[\sum_{j=1}^{m} a_{0j}(\lambda)\exp\left(q_j(\lambda)\hat{\varepsilon}_{xx}t\right)\mathbf{V}_j(\lambda)\right] \times \exp\left[-\frac{D^2\lambda^2}{2}\right]\cos\lambda x\, d\lambda. \tag{C5}$$

If the eigenvalues, eigenvectors and the decomposition of $\mathbf{H}_0$ on this basis have been determined for each wave number λ, the preceding formula allows us to compute $\mathbf{H}$ for a set of values of x and t. Note that, in the limiting case $\lambda = 0$, $q_j(\lambda) = 0$ (Bassi 1986), so that

$$\mathbf{H}_0(t) = \mathbf{H}_0(t=0).$$